sciendo
Austrian Journal of Earth Sciences | Vienna | 2019 | Volume 112/2 | 103 - 124 | DOI: 10.17738/ajes.2019.0007

Palynology, microfacies and ostracods of the Permian–Triassic boundary interval in the Rosengarten/Catinaccio Massif (Southern Alps, Italy)

Hendrik NOWAK[1)]*, Wolfgang METTE[2)], Fabio M. PETTI[3)], Guido ROGHI[4)], Evelyn KUSTATSCHER[1),5),6)]

[1)] Museum of Nature South Tyrol, Bindergasse/Via Bottai 1, 39100 Bozen/Bolzano, Italy; e-mail: hendrik.nowak@naturmuseum.it; evelyn.kustatscher@naturmuseum.it

[2)] Department of Geology, Universität Innsbruck, Innrain 52f, 6020 Innsbruck, Austria; e-mail: wolfgang.mette@uibk.ac.at

[3)] MUSE – Museo delle Scienze di Trento, Corso del Lavoro e della Scienza 3, Trento 38122, Italy; e-mail: fabio.petti@muse.it

[4)] Istituto di Geoscienze e Georisorse - CNR, Via Gradenigo 6, Padova 35131, Italy; e-mail: guido.roghi@igg.cnr.it

[5)] Department of Earth and Environmental Sciences, Paleontology & Geobiology, Ludwig-Maximilians-Universität München, Richard-Wagner-Straße 10, 80333 München, Germany

[6)] SNSB-Bayerische Staatssammlung für Paläontologie und Geologie, Richard-Wagner-Straße 10, 80333 München, Germany

[*)] Corresponding author: Hendrik NOWAK

KEYWORDS upper Permian, Lopingian, Lower Triassic, Dolomites, Bellerophon Formation, Werfen Formation.

Abstract

The Laurinswand section in the Rosengarten/Catinaccio Massif (Dolomites, Southern Alps, Italy) covers the Permian–Triassic boundary in a proximal marine setting. The section has been studied for palynology, ostracods and carbonate microfacies. Five microfacies types are defined for the carbonates of the Bellerophon Formation (Changhsingian) in this section. Ostracod assemblages from the upper Bellerophon Formation show a moderate to high diversity and mostly indicate normal marine conditions, with some samples from the upper Casera Razzo Member being dominated by eurytopic forms. The ostracod fauna follows transgressive-regressive trends with low diverse assemblages occurring in the regressive parts. These trends are also reflected in the microfacies and can be assigned to three sequences. Palynological assemblages are dominated by phytoclasts, which is typical for proximal marine environments. Sporomorphs are represented predominantly by bisaccate and asaccate pollen grains and are mostly minor components of the palynofacies. Other minor, but consistent components in the Bellerophon Formation are acritarchs, *Reduviasporonites* and unidentified possible algae or fungi. The latter are particularly abundant in samples with ostracod faunas indicating restricted conditions. The Werfen Formation (uppermost Permian to Lower Triassic) yielded quantitatively poor palynological assemblages, with one sample from the Tesero Member showing a notable increase in spores and spore tetrads. This is indicative of the so-called "spore spike", a well-known signal from this interval. One sample from the overlying Mazzin Member demonstrated a high relative abundance of *Reduviasporonites*, which may be related to mass occurrences of this taxon in the Tesero Member at Tesero and at other localities near the Permian–Triassic boundary. Such a mass occurrence normally pre-dates the spore spike, whereas at the Laurinswand, the former post-dates the latter considerably.

Das Profil an der Laurinswand im Rosengarten/Catinaccio-Massif (Dolomiten, Südalpen, Italien) umfasst die Perm-Trias-Grenze in einem proximalen, marinen Milieu. Das Profil wurde auf Palynologie, Ostrakodenfaunen und Karbonat-Mikrofazies untersucht. Fünf Mikrofaziestypen wurden für die Karbonate der Bellerophon-Formation (Changhsingium) definiert. Ostrakodenvergesellschaftungen aus der oberen Bellerophon-Formation weisen eine mittlere bis hohe Diversität auf und deuten überwiegend auf normalmarine Bedingungen hin, allerdings werden einige Proben aus dem oberen Casera-Razzo-Member von eurytopen Formen dominiert. Die Ostrakodenfauna folgt transgressiv-regressiven Trends, wobei weniger diverse Faunen in den regressiven Teilen auftreten. Diese Trends sind auch in der Mikrofazies reflektiert und können drei Sequenzen zugeordnet werden. Palynologische Rückstände werden von Phytoklasten dominiert, was typisch für ein proximales, marines Ablagerungsmilieu ist. Sporomorphe sind vor allem durch bisaccate und asaccate Pollenkörner vertreten und sind meist untergeordnete Komponenten der Palynofazies. Weitere untergeordnete, aber stetig auftretende Komponenten in der Bellerophon-Formation sind Akritarchen, *Reduviasporonites* und nicht identifizierte, mögliche Algen oder Pilzreste. Letztere sind besonders häufig in Proben, deren Ostrakodenfauna eingeschränkt marine Bedingungen anzeigt. Die Werfen-Formation (oberstes Perm bis Untertrias) lieferte wenige palynologische Rückstände, wobei eine Probe aus dem Tesero-Member einen bemerkenswerten Anstieg in der Häufigkeit von Sporen und Sporen-Tetraden aufwies. Dies ist ein Hinweis auf den sogenannten „spore spike", ein bekanntes Signal aus diesem Zeitintervall. Eine Probe des darüber liegenden Mazzin-Members beinhaltete eine relativ große Menge an *Reduviasporonites*, was mit Massenvorkommen dieses Taxons nahe der Perm-Trias-Grenze, im Tesero-Member in Tesero und an anderen Orten, zusammenhängen könnte. Ein solches Massenvorkommen liegt normalerweise unterhalb des „spore spike", wohingegen es an der Laurinswand deutlich darüber liegt.

1. Introduction

The most severe mass extinction event in the Phanerozoic occurred at the end of the Permian, ca. 252 million years ago (e.g., Erwin, 1994; Benton and Twitchett, 2003; Benton and Newell, 2014; Chen et al., 2014; Algeo et al., 2015). It is estimated that at least 50 % of families and 80–96 % of species died out during this event (e.g., Raup, 1979; Erwin, 1994; Benton et al., 2004; Knoll et al., 2007). The Southern Alps are one of the key areas for the study of the Permian–Triassic boundary (PTB) and the end-Permian mass extinction (e.g., Twitchett and Wignall, 1996; Twitchett, 1999; Wignall and Twitchett, 2002; Rampino et al., 2002; Koeberl et al., 2004; Farabegoli et al., 2007; Groves et al., 2007; Kearsey et al., 2009; Posenato, 2009, 2010; Brand et al., 2012; Foster et al., 2017) since the boundary interval succession is continuous, fossiliferous, and numerous outcrops representing terrestrial, marine and coastal settings are easily accessible. The PTB interval at the Rosengarten/Catinaccio Massif is not among the reference sections for the Southern Alps but a few profiles were measured and studied in the last 40 years. Massari et al. (1994) presented the lithostratigraphy and petrography of the Lopingian (upper Permian) succession at the Rio Barbide section (at the southern end of the Rosengarten/Catinaccio Massif). Ichnofossils and invertebrates have been studied from the Lower Triassic Werfen Formation in the southern part of the massif (Hofmann et al., 2011, 2015). The Laurinswand section (Figs. 1, 2) in the northern part of the massif has previously been studied for lithostratigraphy, microfacies and carbon isotopes by Boschetti (2010) in an unpublished thesis.

Most studies on PTB sections from the Southern Alps concentrated on the geological, sedimentological, geochemical and some palaeontological studies. Palaeontological studies focussed mainly on bivalves, trace fossils, foraminifera and conodonts (e.g., Twitchett and Wignall, 1996; Twitchett, 1999; Wignall and Twitchett, 2002; Koeberl et al., 2004; Farabegoli et al., 2007; Groves et al., 2007; Kearsey et al., 2009; Posenato, 2009, 2010; Hofmann et al., 2014). Permian–Triassic ostracods were described for the first time from the upper Bellerophon Formation (Changhsingian) of the Rio Barbide and the Digonera sections (Pasini, 1981) and subsequently from the upper Bellerophon and lower Werfen formations at Pufels/Bulla (Crasquin et al., 2008) and from the lower Bellerophon Formation at Seis/Siusi (Mette and Roozbahani, 2012). Palynological studies have been performed in several upper Permian successions of the Southern Alps (Klaus, 1963; Visscher and Brugman, 1986; Massari et al., 1988, 1994; Cirilli et al., 1998; Pittau, 2001; Looy et al., 2005; Spina et al., 2015), but not until now in the Rosengarten/Catinaccio Massif. Detailed palynological analyses from the Werfen Formation covering the PTB interval are only available from Seres (Cirilli et al., 1998) and Tesero (Spina et al., 2015). In addition, spore tetrads from the lower Werfen Formation at Tramin/Termeno were mentioned by Looy et al. (2005). We here report and discuss new results concerning the lithostratigraphy, microfacies, palynology and ostracod assemblages of the Laurinswand section.

2. Geographical and geological setting

The Rosengarten/Catinaccio Massif is located in South Tyrol (northern Italy), east of the city of Bozen/Bolzano, in the westernmost part of the Dolomites (Fig. 1). It is bordered by the Eisacktal/Val Isarco to the northwest, the Tschamintal/Val Ciamin to the north, the Fassatal/Val di Fassa to the east and the Eggental/Val d'Ega to the south and west. Its highest peak is the Kesselkogel/Catinaccio d'Antermoia with 3004 m. The Laurinswand/Croda di Re Laurino is another peak in the central part of the massif and lies southwest of the Kesselkogel. The studied section (46°27'48"N, 11°36'40"E; Fig. 2) is located on the western slope of the Laurinswand, uphill from the Haniger mountain hut (Haniger Schwaige; see also Boschetti, 2010).

During the Permian and Triassic, the Southern Alps were positioned at low latitudes of the northern hemisphere, on the eastern margin of the supercontinent Pangaea close to the Tethys Ocean (Onorevoli and Farabegoli, 2014; Matthews et al., 2016; Torsvik and Cocks, 2017). The late Permian to Early Triassic interval in the Dolomites is represented by the Gröden/Val Gardena Formation (Grödner Sandstein/Arenarie di Val Gardena), Bellerophon Formation and Werfen Formation (Fig. 3). The Gröden/Val Gardena Formation overlies the lower Permian Athesian Volcanic Complex (or Bozen Quartz-porphyry) and consists mostly of fluvial siliciclastic sediments. The onset of the marine Bellerophon Formation represents a transgression of the Tethys Sea, approximately

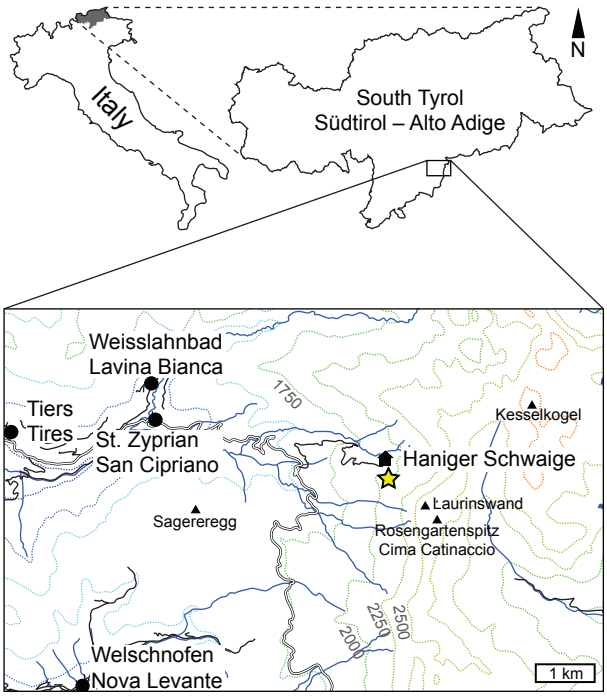

Figure 1: Map showing the position of the Laurinswand section in South Tyrol.

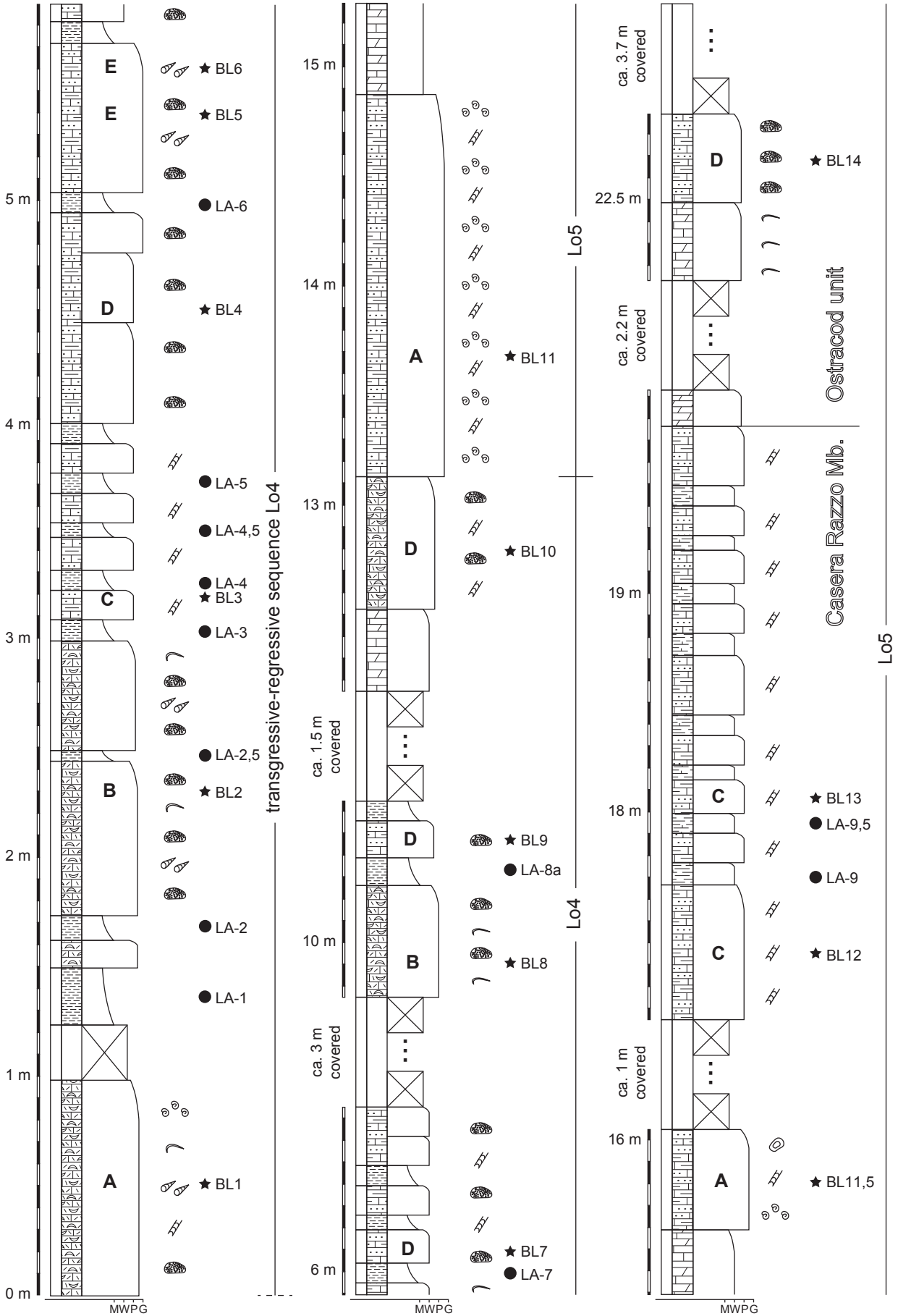

Figure 2: Log of the Laurinswand section with lithostratigraphy, palynomorph and ostracod sampling positions, preliminary results of carbonate microfacies analysis in the Bellerophon Formation and transgressive–regressive sequences.

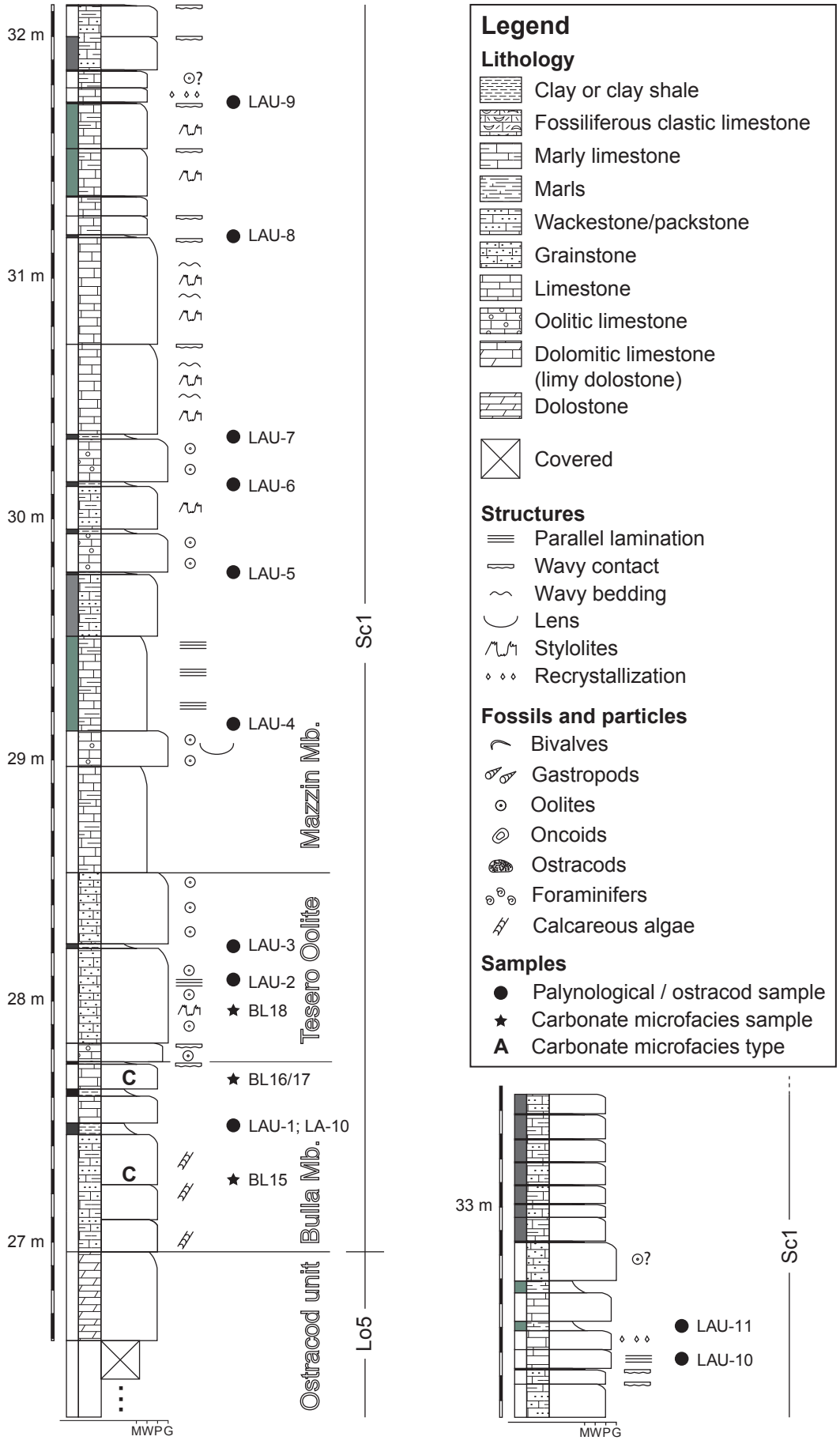

Figure 2: (Continued).

at the Wuchiapingian–Changhsingian boundary (Posenato, 2010). Two facies types of the Bellerophon Formation are distinguished: The "fiemmazza" facies (Massari et al., 1988, 1994; Farabegoli et al., 2007) comprises vuggy dolomites and gypsum, representing a shallow, evaporitic setting, whereas the "badiota" facies contains dark, fossil-rich limestones. The Bellerophon Formation can also be subdivided into the Casera Razzo Member (alternating fossil-rich wacke-/packstones and silts/marls), Ostracod unit (or Ostracod and peritidal dolomite unit, corresponding to the Ostracod Assemblage of Broglio Loriga et al., 1988; silty dolomitic mud-/wackestones

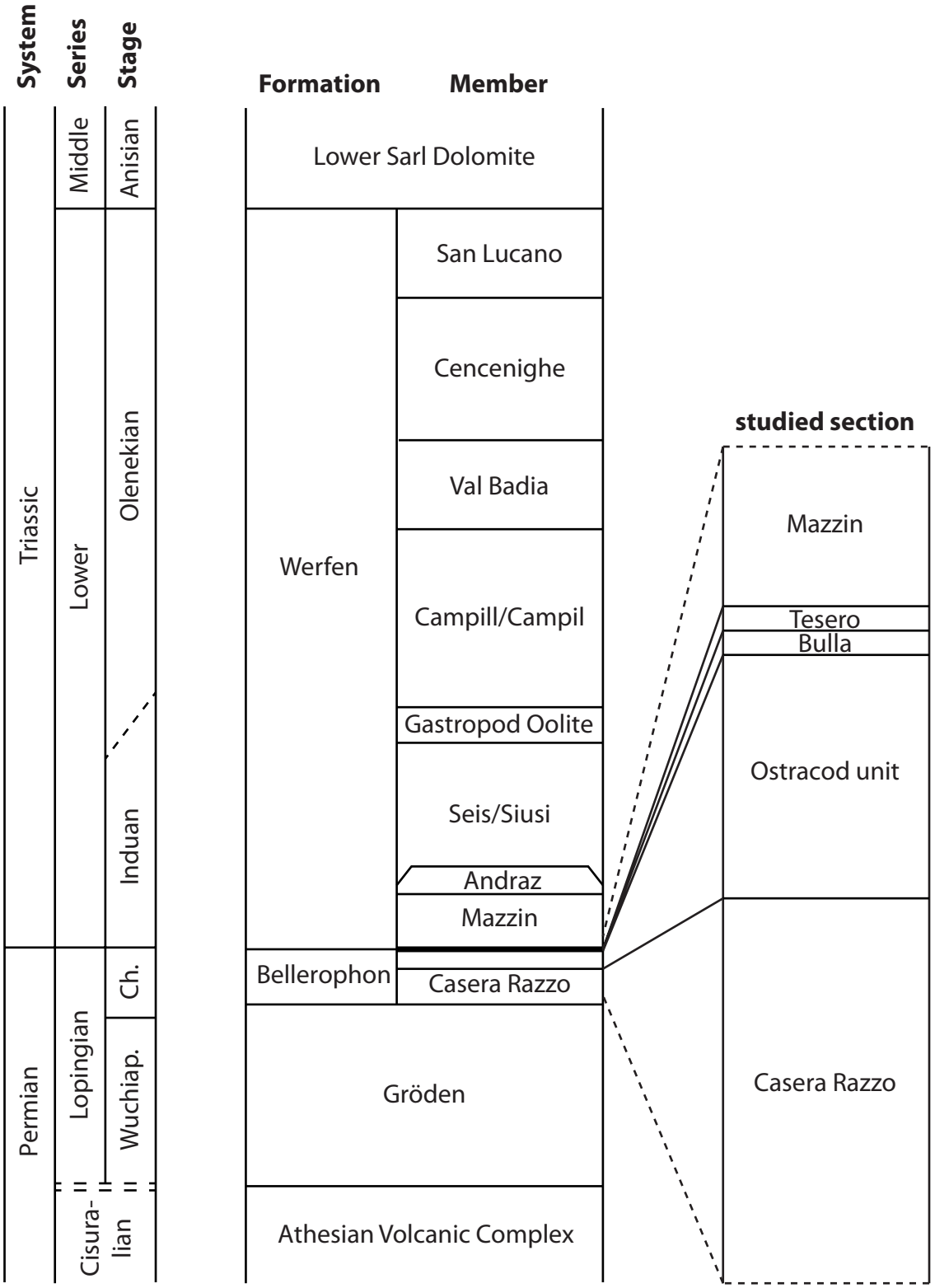

Figure 3: Overview of the upper Permian and Lower Triassic lithostratigraphic units in the Dolomites. Wuchiap. = Wuchiapingian; Ch. = Changhsingian.

with shale interbeds representing a regressive episode) and Bulla Member (up to ca. 1.4 m thick, dark fossiliferous pack-/wackestone with subordinate silts/marls) (Farabegoli et al., 2007; Neri, 2007a).

The Werfen Formation (uppermost Permian–Lower Triassic) in the Southern Alps is subdivided into the Tesero Member (formerly also known as Tesero Oolite or Tesero Horizon; oolitic limestones), Mazzin Member (mud-/wacke-/packstones), Andraz Member (formerly Andraz Horizon; peritidal marly-silty dolomites), Seis/Siusi Member (limestones and silty marlstones), Gastropod Oolite Member (gastropod-rich tempestite layers and conglomerates), Campill/Campil Member (predominantly sandstones, siltstones and marls), Val Badia Member (peri- to subtidal marly dolomites and limestones), Cencenighe Member (oolitic-bioclastic calcarenites and sandstones) and San Lucano Member (sub- to supratidal sand-/siltstones, marls, calcarenites and dolomites) (Broglio Loriga et al., 1990; Neri, 2007b; Brandner et al., 2009). The Tesero and Mazzin members are partly contemporaneous and interfingering. The Werfen Formation is succeeded by the Anisian Lower Sarl Dolomite or unconformably overlain by the Richthofen conglomerate (Broglio Loriga et al., 1990; Neri, 2007b).

3. Materials and methods

The lower part of the Laurinswand section (Bellerophon Formation) was sampled in 2008 and 2009 for microfacies (sample number prefix BL), ostracods and palynomorphs (prefix LA) (Fig. 2). Microfacies samples were taken from limestone beds, while samples for ostracods and palynomorphs were collected from shales. In 2016, eleven additional palynological samples (prefix LAU) were taken from shales, marls and thinly bedded limestone in the uppermost Bellerophon Formation (one sample), the Tesero Member (two samples) and the Mazzin Member (eight samples). The first field work campaign took place in a creek with changing and discontinuous outcrop conditions, the second concentrated on a nearby rockface on the slope above the Haniger mountain hut.

For microfacies analyses, thin sections were produced from the rock samples. Ostracods were extracted using hydrogen peroxide (15%). The 24 palynological samples were macerated with hydrofluoric and hydrochloric acids using a standard protocol and filtered at 150 µm and 15 or 10 µm. Residues were mounted on permanent slides using Canada balsam or the Eukitt® mounting medium. Photographs of palynomorphs were taken with a Leica DMC4500 camera mounted on a Leica DM 2500 LED microscope in transmitted light or under fluorescent light.

4. Results

4.1 Lithostratigraphy

In the Laurinswand section (Fig. 2), the outcropping part of the Casera Razzo Member of the upper Bellerophon Formation is 27 m thick. It is dominated by wacke- and packstones with subordinate marls. Several beds are dolomitized. The most prominent biogenic components are gymnocodiacean algae (Fig. 4A–B, D–E), ostracods (Fig. 4C, F–G; Fig. 5), bivalves (Fig. 4C, F), gastropods (Fig. 4A–B, G), and foraminifers (Fig. 4A–B). The lowermost portion of the section (3 m) is made up of bioclastic packstones and grainstones with algal fragments (Gymnocodiaceae), gastropods, foraminifers and ostracods. Within this interval, thin layers of dark-grey marly coquinas occur. Upwards, the section continues with 1 m of packstones with Gymnocodiaceae alternating with marls and marlstones, followed by about 2 m of packstones rich in gastropods and ostracods and 1 m of ostracod/gastropod wackestones alternating with thin layers of marlstone rich in mollusc shells and Gymnocodiaceae. Subsequently, the section is covered for about 3 m and resumes with about 0.5 m of mollusc packstones with ostracods and thin-layered ostracod wackestones and packstones. Following another covered interval of about 1.5 m, the section continues with light grey dolomitic limestones and ostracod wackestones and packstones (1 m), which is overlain by 1 m of packestones and grainstones with abundant intraclasts, calcareous algae and foraminifers (Fusulinina, Miliolina). Upwards follow 3 m of brownish-beige dolomitic limestones and bioclastic packstones and grainstones with oncoids, algae (Dasycladaceae) and foraminifers (Miliolina). Upsection, above a covered interval of ca. 1 m, the succession continues with about 2.5 m of wackestones and packstones with Gymnocodiaceae and marlstone interlayers. The Ostracod unit is interrupted by several covered intervals, with the outcropping part showing brownish bioclastic dolostones, ostracod packstones and beige marly bioturbated dolostones and dolomitic marls.

The Bulla Member is less than one metre thick and comprises Gymnocodiaceae wacke-/packstones (Fig. 4D–E), which at the top of the member are rich in peloids and fusulinid foraminifers. The boundary with the overlying Tesero Member of the Werfen Formation (0.8 m thick) is sharp and marked by the occurrence of thick-bedded oolitic grainstones (Fig. 4H). The lowermost portion of the Mazzin Member of the Werfen Formation (1 m) is characterized by laminated marly limestones alternated with thick-bedded oolitic limestones. The overlying part (2 m) is made of oolitic wacke-/packstones with wavy flaser bedding. Oolites almost completely disappear in the uppermost part represented by wavy bedded wacke-/packstones and grainstones.

4.2 Carbonate microfacies analysis

Five microfacies (MF) types are distinguished in the limestones of the Casera Razzo Member, one of which (MF type C, see 4.2.3) also occurs in the Bulla Member.

4.2.1 MF type A (Bioclast-Intraclast Grain-/Packstone)

This microfacies type is recorded by the samples BL1, BL11 and BL11.5 (Fig. 2, Fig. 4A–B). It shows a relatively high diversity of organisms including

echinoderm fragments, gastropods, ostracods, fusulinid and miliolinid foraminifers (*Nankinella*, *Globivalvulina*, *Hemigordius*), Textulariina (*Glomospirella*), various Lagenina (Nodosariidae), Gymnodiaceae (*Gymnocodium bellerophontis*) and few Dasycladaceae. Most of the bioclasts are abraded. Some shells show borings and

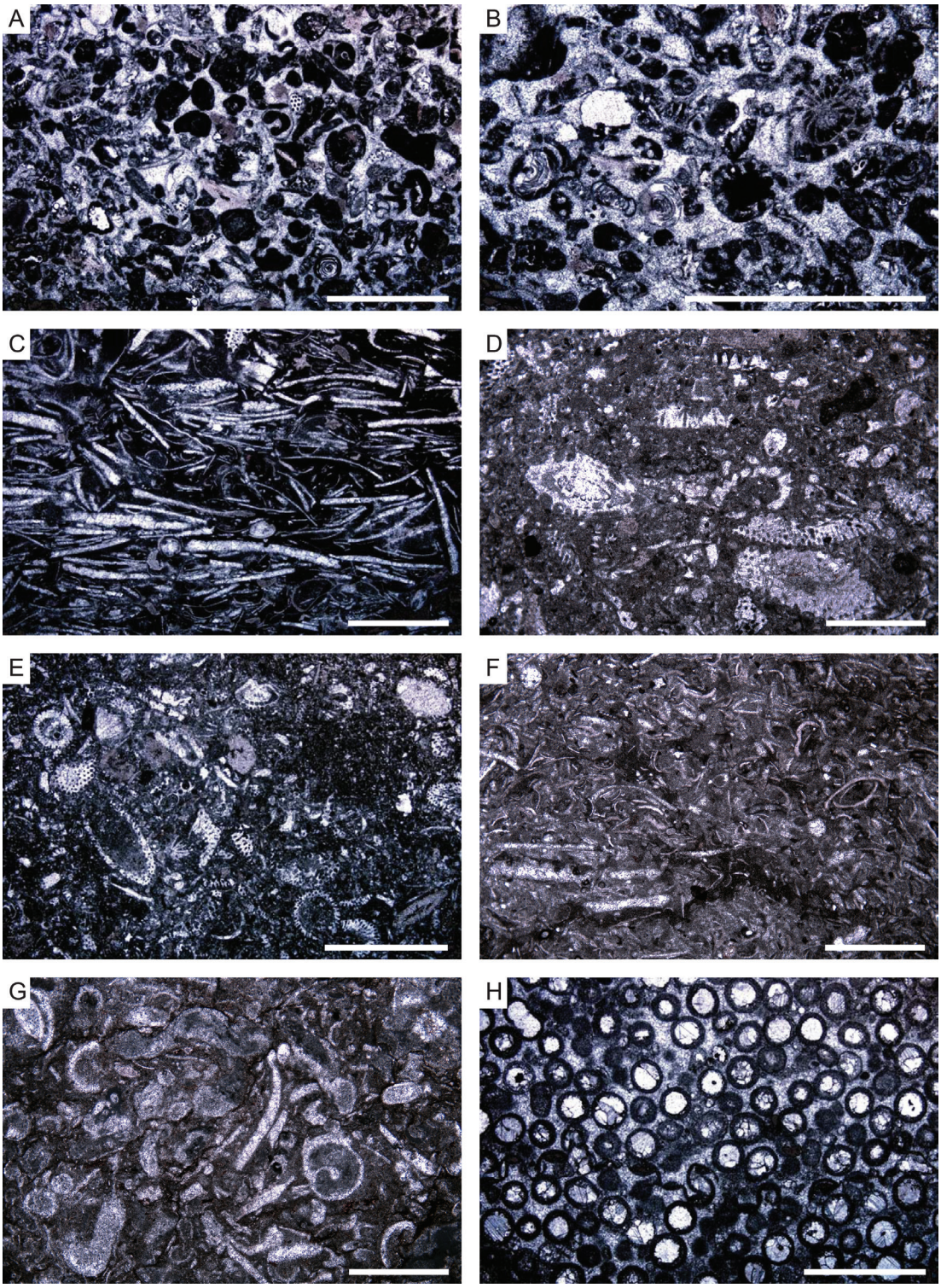

Figure 4: Characteristic carbonate microfacies types of the Bellerophon Formation and the Tesero Member of the Werfen Formation at the Laurinswand section. Scale bars = 2 mm. **A, B**, MF type A: Pack-/grainstone with intraclasts, calcareous algae, foraminifers (Fusulinina, Miliolina) and gastropods, sample BL11. **C**, MF type B: Bioclastic packstone with ostracods and fragments of mollusc shells, sample BL2. **D**, MF type C: Gymnodiaceae packstone with fragments of *Gymnocodium bellerophontis*, Fusulinida (*Nankinella*) and Dasycladaceae (*Mizzia*), sample BL15, Bulla Member. **E**, MF type C: Gymnodiaceae pack-/wackestone, sample BL15 (same sample as D). **F**, MF type D: Ostracod packstone with disarticulated ostracods and fragments of mollusc shells, with some shell fragments showing borings and encrustations of sessile foraminifers, sample BL14. **G**, MF type E: Gastropod-Ostracod-Foraminifer packstone with fragmented gastropod shells and disarticulated ostracods, sample BL5. **H**, Oolithic grainstone in the Tesero Member, sample BL18.

encrustations by sessile foraminifera. The fusulinid tests are mostly reworked. Intraclasts with reworked bioclasts do also occur.

The high abundance of bioclasts of euhaline organisms such as echinoderms, fusulinid foraminifers and Nodosariidae in MF type A indicates normal marine conditions. According to the sediment texture and the high abundance of abraded bioclasts and biogenic encrustations, MF type A is interpreted as bioclastic sand shoal deposits in a highly turbulent open marine environment. The sedimentation rate was probably very low. This MF type corresponds to the Ramp Microfacies Type (RMF) 26 *sensu* Flügel (2004).

4.2.2 MF type B (Mollusc-Ostracod Pack-/Wackestone)

MF type B is represented by samples BL2 and BL8 (Fig. 2, Fig. 4C). The bioclastic components in this microfacies type are ostracods and poorly sorted shell concentrations of fragmented bivalves and gastropods. The ostracods are articulated or disarticulated. Some of the mollusc shells show borings and thin micritic crusts. Euhaline organisms such as echinoderms or fusulinid foraminifers are absent. Shell concentrations may occur in various shelf environments (Flügel, 2004). The low diversity of bioclast assemblages and absence of euhaline organisms in MF type B is indicative for a restricted and shallow lagoonal depositional environment. MF type B is therefore interpreted as proximal storm deposits.

4.2.3 MF type C (Gymnodiaceae Packstone)

MF type C is the most abundant microfacies type in the upper Bellerophon Formation at the Laurinswand section and is represented by samples BL3, BL12, BL13, BL15, BL16 and BL17 (Fig. 2, Fig. 4D–E). The most abundant organisms are Gymnodiaceae (*Gymnocodium bellerophontis*, *Permocalculus* sp.), which are associated with miliolinid foraminifers dominated by *Hemigordius*. In most samples, the miliolinids occur together with Fusulinina (*Nankinella*, *Globivalvulina*) and/or Lagenina and Textulariina (*Glomospira*, *Glomospirella*). Less abundant are Dasycladaceae (*Atractyliopsis*, *Mizzia*). Minor bioclastic components are ostracods and echinoderm fragments.

Fusulinid and most nodosariid foraminifers are adapted to open marine environments and are generally not recorded in dolomitic or evaporitic deposits of the Bellerophon Formation (Noé, 1987). The occurrence of Fusulinina and Nodosariida in several, but not all samples of MF type C suggests that this microfacies type represents a transitional zone between restricted and open lagoonal conditions. It is comparable to RMF) type 20 (Bioclastic Wackestone/Packstone with algae and benthic foraminifera) *sensu* Flügel (2004).

4.2.4 MF type D (Ostracod Pack-/Wackestone)

Microfacies type D is recorded by the samples BL4, BL7, BL9, BL10 and BL14 (Fig. 2, Fig. 4F). It is one of the most abundant microfacies type in the upper Bellerophon Formation at Laurinswand section and shows mass accumulations of disarticulated ostracod shells. In some samples, the ostracods are associated with calcareous algae (Gymnodiaceae, Dasycladaceae: *Atractyliopsis*) and fragmented or reworked gastropod shells. Euhaline organisms do not occur.

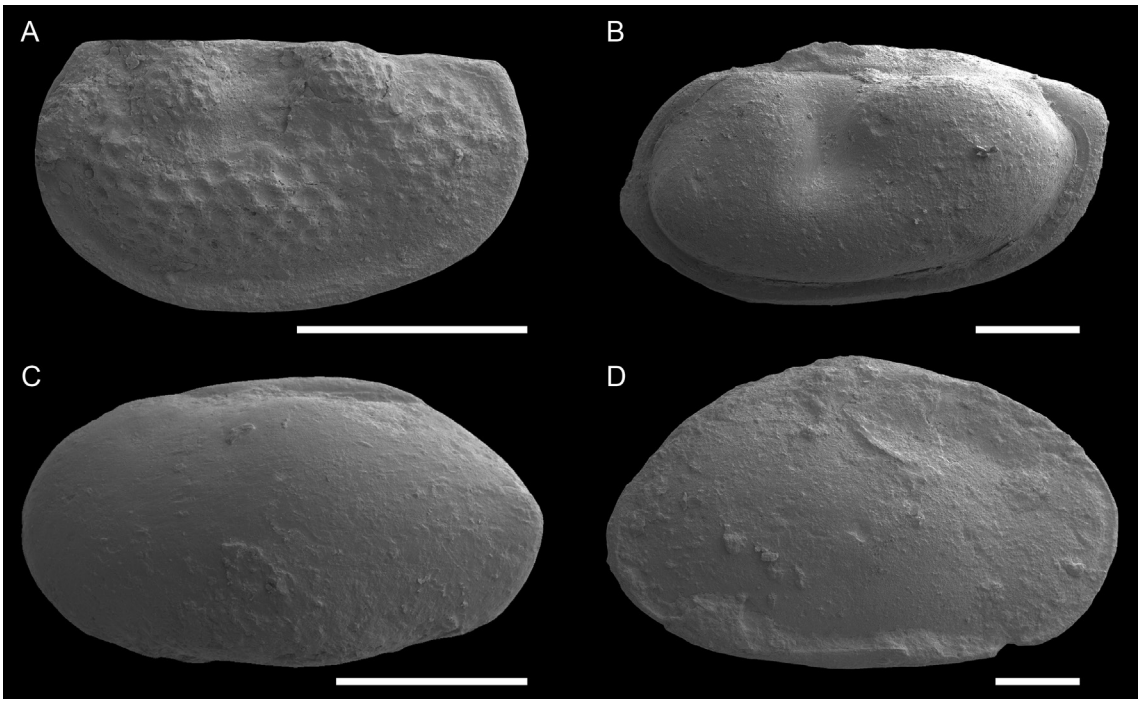

Figure 5: Typical ostracods from the upper Bellerophon Formation at the Laurinswand section. Scale bars = 200 µm. **A**, *Neoulrichia pulchra* Kozur 1981, left valve, sample LA-3. **B**, *Sargentina postacuta* (Zalànyi 1974), carapace, left lateral view, sample LA-4. **C**, *Cavellina bellerophonella* Crasquin 2008, carapace, left lateral view, sample LA-2. **D**, *Cryptobairdia bellerophonella* Mette and Roozbahani 2012, carapace, right lateral view, sample LA-6.

The very low diversity of represented fossil groups and absence of echinoderms and foraminifers suggest a restricted and shallow lagoonal environment. The absence of articulated ostracod shells points to high water turbulence and transport. MF-Type D is thus interpreted as a storm deposit of the inner ramp.

4.2.5 MF type E (Gastropod-Ostracod-Foraminifer Packstone)

The bioclasts of MF type E are dominated by gastropods, fragments of bivalve shells, articulated and disarticulated ostracods and miliolinid foraminifers (*Hemigordius*). Few fragments of calcareous algae (Gymnodiaceae, Dasycladaceae) do also occur. Intraclasts are relatively abundant. This microfacies type is represented by samples BL5 and BL6 (Fig. 2, Fig. 4G).

The composition and low diversity of the fossil assemblages of MF type E are indicative of a shallow marine, restricted environment. This interpretation is particularly supported by the low diversity of foraminifers, which are exclusively represented by the Miolioliina (*Hemigordius*). *Hemigordius* is interpreted as a marine euryhaline foraminifer due to its occurrence in evaporitic deposits of the Bellerophon Formation, intertidal deposits of the Tesero Member and in biosparitic limestones of open marine facies (Noé, 1987). The occurrence of intraclasts suggests that the protected environment was affected by periods of high water turbulence and reworking, probably during storm events. MF type E is comparable to RMF type 16 (Mudstone, wackestone or packstone with abundant miliolid foraminifera) (Flügel, 2004) and was deposited in a restricted inner ramp setting.

4.3 Palynomorphs

Most samples from the Bellerophon Formation yielded rich palynological assemblages (Fig. 6, 7, Tab. 1) with abundant taeniate and non-taeniate bisaccate pollen (e.g., *Jugasporites* Leschik 1956, Fig. 6J, K; *Klausipollenites* Jansonius 1962, Fig. 6G; *Lunatisporites* Leschik 1956, Fig. 6F; *Illinites* Kosanke 1950, Fig. 7L; *Falcisporites* Leschik 1956; *Lueckisporites* Potonié et Klaus 1954, Fig. 6H). Asaccate pollen (*Vittatina* Wilson 1962; *Ephedripites* Bolchovitina ex Potonié 1958, Fig. 6N; *Cycadopites* Wodehouse, 1933, Fig. 6M) and spores (*Playfordiaspora* Maheshwari et Banerji 1975, Fig. 6D; *Lycospora* Schopf et al. 1944, Fig. 6C; *Densosporites* Berry 1937; *Kraeuselisporites* Leschik 1956; *Calamospora* Danzé-Corsin et Laveine 1963, Fig. 6A; *Converrucosisporites* Klaus 1963, Fig. 6B) are comparatively rare. Monosaccate prepollen (*Nuskoisporites* Potonié et Klaus 1954, Fig. 6E) and trisaccate or trilobate pollen (one unidentified, possibly aberrant grain) are very rare. A consistently present component is *Reduviasporonites chalastus* (see 5.3), a problematic organic-walled microfossil taxon that occurs as single cells (Fig. 8M) or occasionally branching chains of cells (Fig. 7M). It is usually the best preserved component in a palynological assemblage. Most palyniferous samples from the Bellerophon Formation include low numbers of acritarchs (predominantly *Leiosphaeridia* Eisenack 1958, Fig. 7L; *Veryhachium* Deunff 1954, Fig. 7I; *Micrhystridium* Deflandre 1938, Fig. 7C, F), and most samples contain an unidentified type of probable multicellular algae (or fungal remains; Fig. 7D, E, G, H, J, K). These putative algae occur as variable-sized, loose and disorderly clusters that sometimes appear to consist of filaments. Individual cells have a circular or slightly ovoid outline, with diameters of 3–22 µm. Under transmitted light, the cellular structures tend to be inconspicuous to indiscernible, but they are more or less clearly visible under fluorescent light. These structures show relatively strong fluorescence, in contrast to most other components in these assemblages apart from sporomorphs and acritarchs. The putative algae are generally rare, but occur in considerable relative abundance in samples LA-8a and LA-9,5. This type of microfossil is absent in samples from the Werfen Formation. By contrast, the latter yielded sporadic specimens of *Cymatiosphaera* Wetzel 1933, a prasinophycean green alga that was not found in the Bellerophon Formation. Common in the Bellerophon Formation and very rare in the Werfen Formation is *Brazilea* (al. *Spheripollenites*) *balmei* (Jansonius 1962) Grenfell 1995 (Fig. 6O). This species was originally described by Jansonius (1962) as a type of conifer pollen (*Spheripollenites* Couper 1958), but was identified by Grenfell (1995) as spores of zygnemataceae algae and assigned to *Brazilea* Tiwari et Navale 1967. All samples from the Bellerophon Formation yielded at least some well-preserved palynomorphs, but the bulk of the grains shows mechanical and diagenetic damage, with deformed grains often showing numerous imprints of crystals. Sacci of pollen are frequently found detached from the corpus.

Samples from the Werfen Formation produced quantitatively poor assemblages (Fig. 8, Tab. 1), which however always contain a few well-preserved palynomorphs (bisaccate pollen grains; spores; *Reduviasporonites chalastus*, Fig. 8M; *Cymatiosphaera* sp., Fig. 8N, O; *Brazilea balmei*, Fig. 8K). Pollen and spores are of limited diversity compared to the Bellerophon Formation. Identified taxa are *Klausipollenites schaubergeri* (Potonié et Klaus 1954) Jansonius 1962 (Fig. 8E, F), *Cycadopites* sp., *Ephedripites* sp. (Fig. 8J), *Falcisporites* ex gr. *F. zapfei* (Potonié et Klaus 1954) Leschik 1956 (Fig. 8I), *Platysaccus* sp., ?*Protohaploxypinus* sp. (Fig. 8H), *Vitreisporites* sp., *Stroterisporites* sp. cf. *S. richteri* (Klaus 1955) Wilson 1962 (Fig. 8G), ?*Densosporites* sp. (Fig. 8C), *Lundbladispora* sp. and *Lycospora* sp. (Fig. 8D). Notably, both samples from the Tesero Member yielded spore tetrads (Fig. 8A, B), as well as a conspicuously higher amount of spores compared to the Bellerophon Formation (which is however not quantified due to low overall yield).

4.4 Palynofacies

Palynofacies assemblages (Fig. 9, 10) are dominated by terrestrial phytoclasts (Fig. 7A, 8L) in various states of degradation. Amorphous organic matter (AOM) is a rare to common (1–16%, except for LA-7 with ca. 40%)

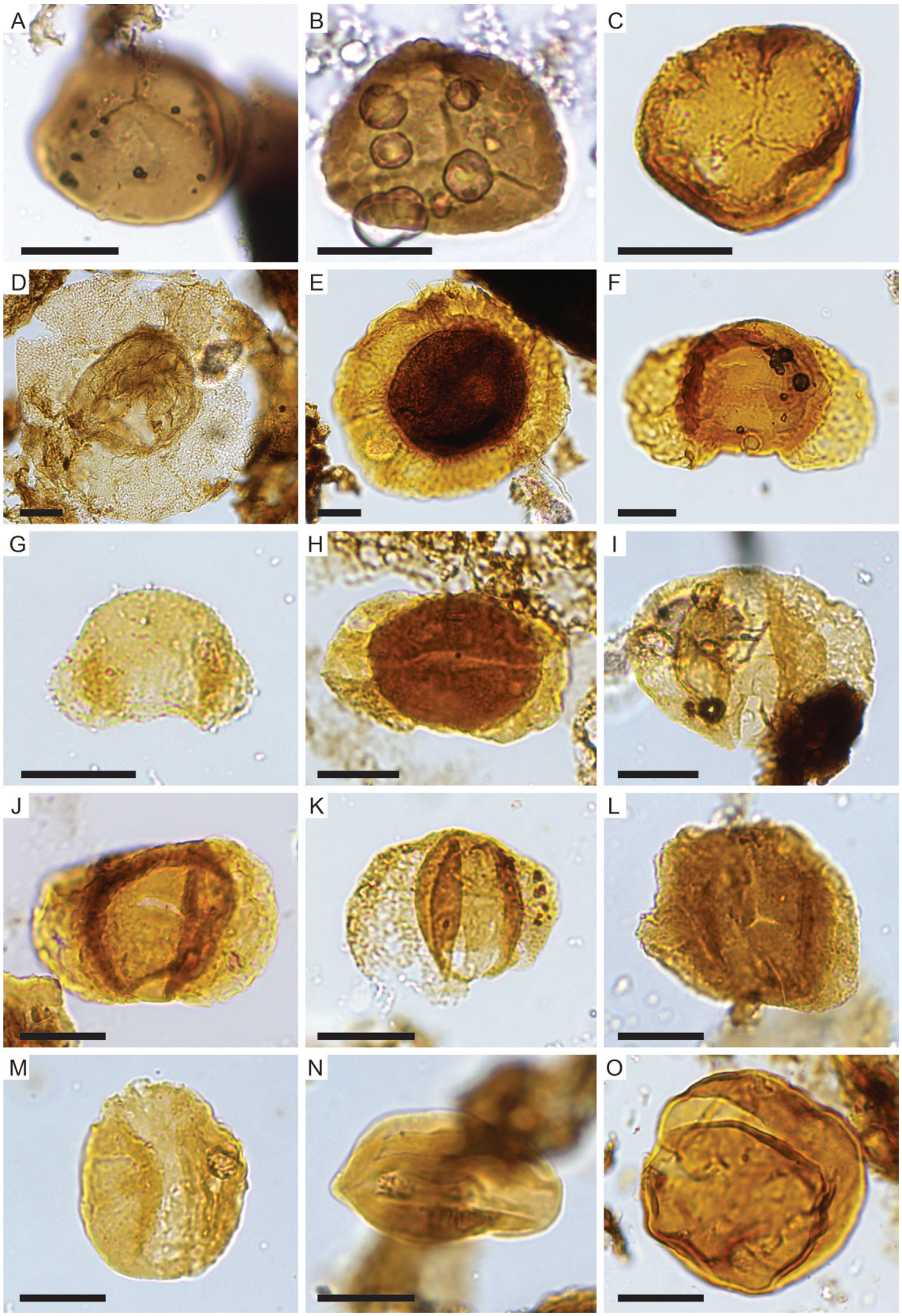

Figure 6: Spores and pollen from the Bellerophon Formation at the Laurinswand section. Scale bars = 20 µm. Sample numbers followed by slide numbers and England Finder Graticule coordinates. **A**, *Calamospora* sp., sample LA-3(3), Q35. **B**, *Converrucosisporites dejerseyi* Klaus 1963, sample LA-3(3), P41/1. **C**, *Lycospora* sp., sample LA-8a(3), D29. **D**, *Playfordiaspora crenulata* (Wilson 1962) Foster 1979, sample LA-3(1), N41/3-O41/1. **E**, *Nuskoisporites dulhuntyi* Potonié et Klaus 1954, sample LA-4(4), J41/4. **F**, *Lunatisporites labdacus* (Klaus 1963) Visscher 1971, sample LA-8a(3), L27. **G**, *Klausipollenites schaubergeri* (Potonié et Klaus 1954) Jansonius 1962, sample LA-4(3), L38/1. **H**, *Lueckisporites virkkiae* Potonié et Klaus 1954, sample LA-7(3), H38/2. **I**, *Paravesicaspora splendens* (Leschik 1956) Klaus 1963, sample LA-4(1), G36/3. **J**, *Jugasporites paradelasaucei* Klaus 1963, sample LA-1(4), K32/2-K33/1. **K**, *Jugasporites delasaucei* (Potonié et Klaus 1954) Klaus 1963, sample LA-5(2), U40/4. **L**, *Illinites parvus* Klaus 1963, sample LA-2,5(1), T31/2. **M**, *Cycadopites* sp., sample LA-4(1), L36/2. **N**, *Ephedripites* sp. cf. *E. steveesii* Jansonius 1962, sample LA-4(1), R39/4. **O**, *Brazilea balmei* (Jansonius 1962) Grenfell 1995, sample LA-8a(4), R40/1-2.

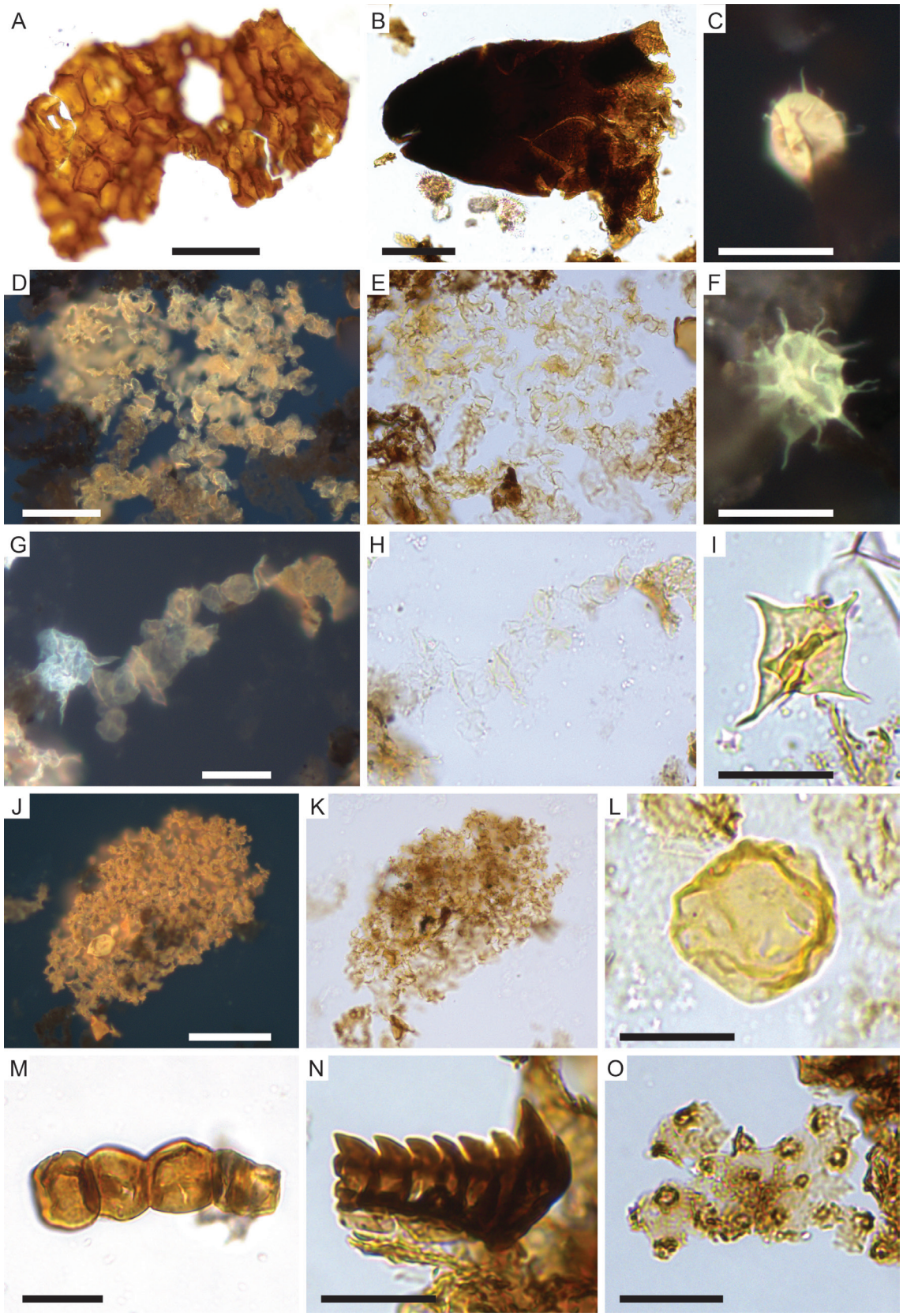

Figure 7: Other palynomorphs from the upper Bellerophon Formation at the Laurinswand section. Scale bars = 50 µm for A, B, G, H, J, K, all other scale bars = 20 µm. Sample numbers followed by slide numbers and England Finder Graticule coordinates. **A**, plant cuticle fragment, sample LAU-1(155 µm), V43/1. **B**, phytoclast, sample LA-4(2), L36/2. **C**, *Micrhystridium* sp., sample LA-10(2), S32/2. **D, E**, possible algae, sample LA-8a(3), E31/1-2. D, fluorescence. E, transmitted light. **F**, *Micrhystridium* sp., sample LA-2,5(1), K39/3. **G, H**, possible algae and *Veryhachium* sp. (*lairdii* group *sensu* Servais et al., 2007), sample LA-8a(4), W31/4. G, fluorescence. H, transmitted light. **I**, *Veryhachium nasicum* (Stockmans et Willière 1960) Stockmans et Willière 1962, sample LA-2(1), H39. **J, K**, possible algae, sample LA-8a(4), W30/4. J, fluorescence. K, transmitted light. **L**, *Leiosphaeridia* sp., sample LA-8a(2), U38/2. **M**, *Reduviasporonites chalastus* (Foster 1979) Elsik 1999, sample LA-9,5(3), J43/4-K43/2. **N**, scolecodont, sample LA-4(2), R35/3. **O**, animal (possible worm) cuticle, sample LA-4(2), R35/3.

Palynomorph taxa	LA-												LAU-										
	1	2	2,5	3	4	4,5	5	7	8a	9	9,5	10	1	2	3	4	5	6	7	8	9	10	11
	Casera Razzo											Bulla	Tesero			Mazzin							
?Gardenasporites sp.	X																						
Deltoidospora sp.	X																						
Favisporites lucidus Leschik 1956	X																						
Vittatina sp.	X	X																					
Jugasporites delasaucei (Potonié et Klaus 1954) Leschik 1956	X				X		X																
Striatoabieites sp.	X	?					X	X															
Illinites spp.	X		X	X	X				X														
Falcisporites nutallensis (Clarke 1965) Balme 1970	X	X	X	X					X														
Paravesicaspora splendens (Leschik) Klaus 1963	X	X	X	?	X	X	X		X														
Lunatisporites labdacus (Klaus)	X			X					X		X												
Jugasporites paradelasaucei Klaus 1963	X				X				X		X												
Playfordiaspora crenulata (Wilson) Foster 1979	X	X		X	X		X		X	X	X	?											
Platysaccus papilionis Potonié et Klaus 1954	X	?	X		X	?			X		X	X											
Lueckisporites virkkiae Potonié et Klaus 1954	X	X	X	X	X	X	X	X	X	X	X	X	X										
Lueckisporites spp.	X			X			X		X			X	X										
Jugasporites spp.	X	X	X	X	X	X	X	X	X		X		X										
Cycadopites spp.	X	X		X	X		X		X			X	X		X				X				
Platysaccus sp.	X	X		X	X	X			X		X	X								X			
Lycospora spp.	X								X														X
Klausipollenites schaubergeri (Potonié et Klaus) Jansonius 1962	X	X	X	X	X	X	X	X	X	X	X	X	X		X			X			X	X	X
Falcisporites spp.		X									X		?										?
Falcisporites zapfei (Potonié et Klaus) Leschik 1956		X		X	X		X		X		X		?		X								X
Jugasporites lueckoides Klaus 1963		X			X																		
Klausipollenites sp. cf. *K. staplinii* Jansonius 1962		X						X															
Protohaploxypinus sp. cf. *P. microcorpus* (Schaarschmidt) Clarke 1965		X					X	X	X	X													
Lunatisporites sp.		X			X				X		X												
Vitreisporites sp.		X		?			?				X	X						?					
Klausipollenites vestitus Jansonius 1962		X	X										X								X		
Converrucosisporites eggeri Klaus 1963			X																				
Illinites parvus Klaus 1963			X				X			X		X											
Klausipollenites spp.			X	X	X	X			X				X										
Densosporites spp.				?		X									X								
Converrucosisporites dejerseyi Klaus 1963				X																			
Favisporites tenuis Leschik 1956				X																			
Calamospora sp.				X		X	?			X													
Nuskoisporites dulhuntyi Potonié et Klaus 1954				X	X		X			?	X												
Illinites pemphicus Klaus 1963					X																		
Jugasporites schaubergeroides Klaus 1963					X				X		X	X											
Ephedripites sp. cf. *E. stevesii* Jansonius 1962					X										X								
Strotersporites sp. cf. *S. richteri* (Klaus 1955) Wilson 1962					X			X											X			?	
Strotersporites wilsonii Klaus 1963							X																
Kraeuselisporites sp.							X																
Limitisporites sp.							X																
Illinites gamsi Klaus 1963							X		X														
Araucariacites sp.								X															
Lunatisporites sp. cf. *L. ortisei* (Klaus) Góczán 1987								X	X		X												
Lueckisporites parvus Klaus 1963								X				X											
Lunatisporites alatus (Klaus 1963) Pittau in Massari et al. 1988									X														
Vittatina sp. cf. *V. costabilis* Wilson 1962									X														
Leiotriletes sp.										X													
Lundbladispora sp.															X	?	X						
?Protohaploxypinus sp.																	X						
tetrads		X												X	X								
Reduviasporonites chalastus (Foster 1979) Elsik 1999	X	X	X	X	X	X	X	X	X	X	X	X	X		X	?	X	X		X	X	X	X
?algae	X		X	X	X		X	X	X	X	X	X	X										
Brazilea balmei (Jansonius 1962) Grenfell 1995	X		X	X	X		X	X	X	X	X												X
Cymatiosphaera sp.															X					X			X
Micrhystridium spp.	X	X	X		X	X	X	X	X	X		X	X										
Veryhachium lairdii group *sensu* Servais et al. (2007)	X	X	X	?	X	?		X	X		X		?										
Leiosphaeridia spp.	X		X	X	X	X	X	X	X	X	X	X	X										

Table 1: Palynomorph range chart of the upper Bellerophon and lower Werfen formations at the Laurinswand section.

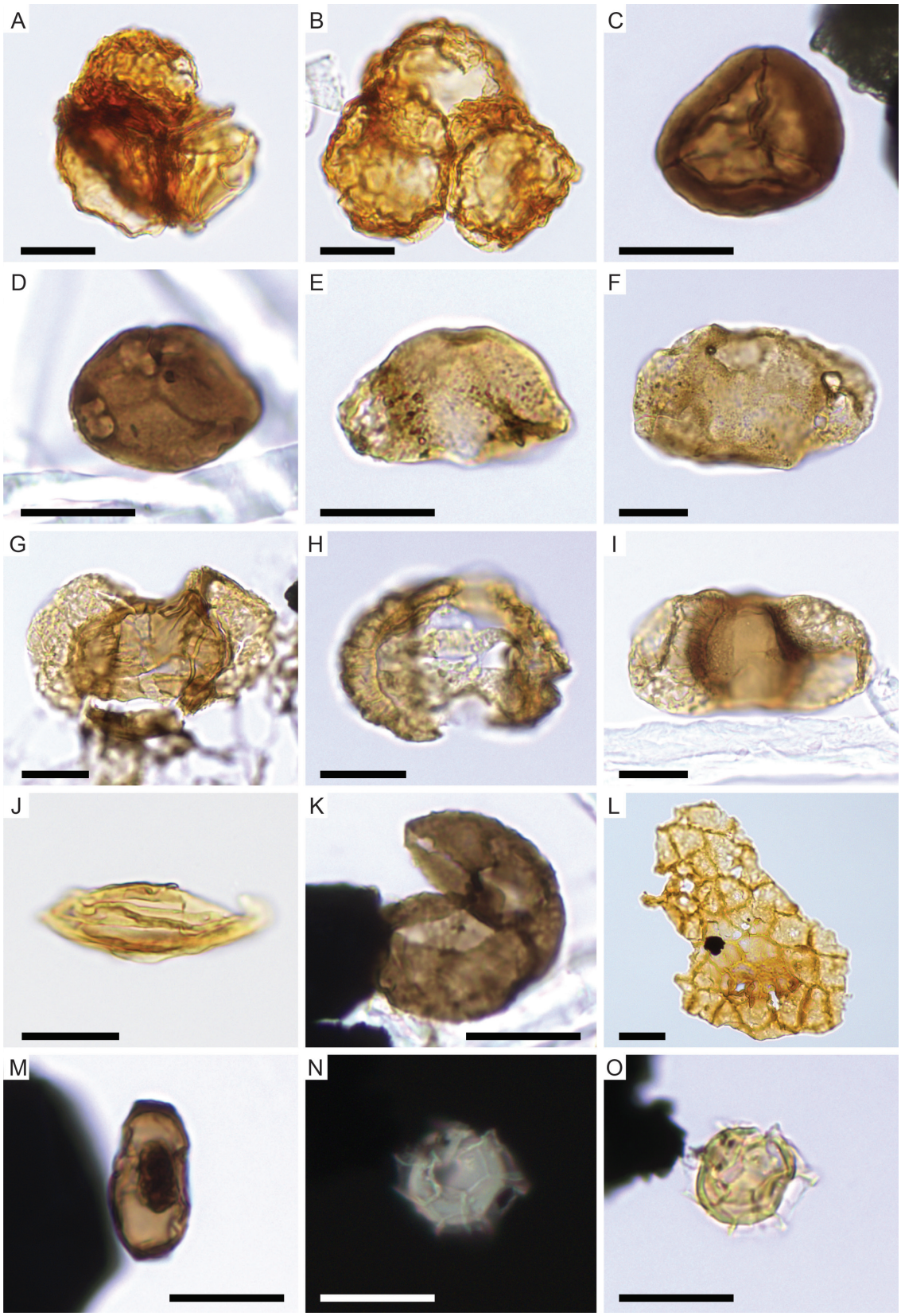

Figure 8: Palynomorphs from the lower Werfen Formation at the Laurinswand section. Scale bar = 50 µm for L, all other scale bars = 20 µm. Sample numbers followed by slide numbers and England Finder Graticule coordinates. **A, B**, spore tetrads indet. A, sample LAU-2(1), S33/4. B, sample LAU-3(1), Q42. **C**, *Densosporites* sp., sample LAU-3(1), H41/2-H42/1. **D**, *Lycospora* sp., sample LAU-11(1), Q38/3. **E, F**, *Klausipollenites schaubergeri* (Potonié et Klaus 1954) Jansonius 1962. E, sample LAU-10(1), S39/1. F, sample LAU-6(1), V37/3. **G**, *Strotersporites* sp. cf. *S. richteri* (Potonié et Klaus 1954) Jansonius 1962, sample LAU-7(1), Q35/3. **H**, ?*Protohaploxypinus* sp., sample LAU-5(1), Q42/4. **I**, *Falcisporites zapfei* (Potonié et Klaus 1954) Leschik 1956, sample LAU-11(1), K38/1-2. **J**, *Ephedripites* sp., sample LAU-3(1), T38/1. **K**, *Brazilea balmei* (Jansonius 1962) Grenfell 1995, sample LAU-11(1), T36/1. **L**, plant cuticle fragment, sample LAU-2(1), V36/4. **M**, *Reduviasporonites chalastus* (Foster 1979) Elsik 1999, sample LAU-5(1), S36/2. **N, O**, *Cymatiosphaera* sp., sample LAU-3(1), O39/4. N, fluorescence. O, transmitted light.

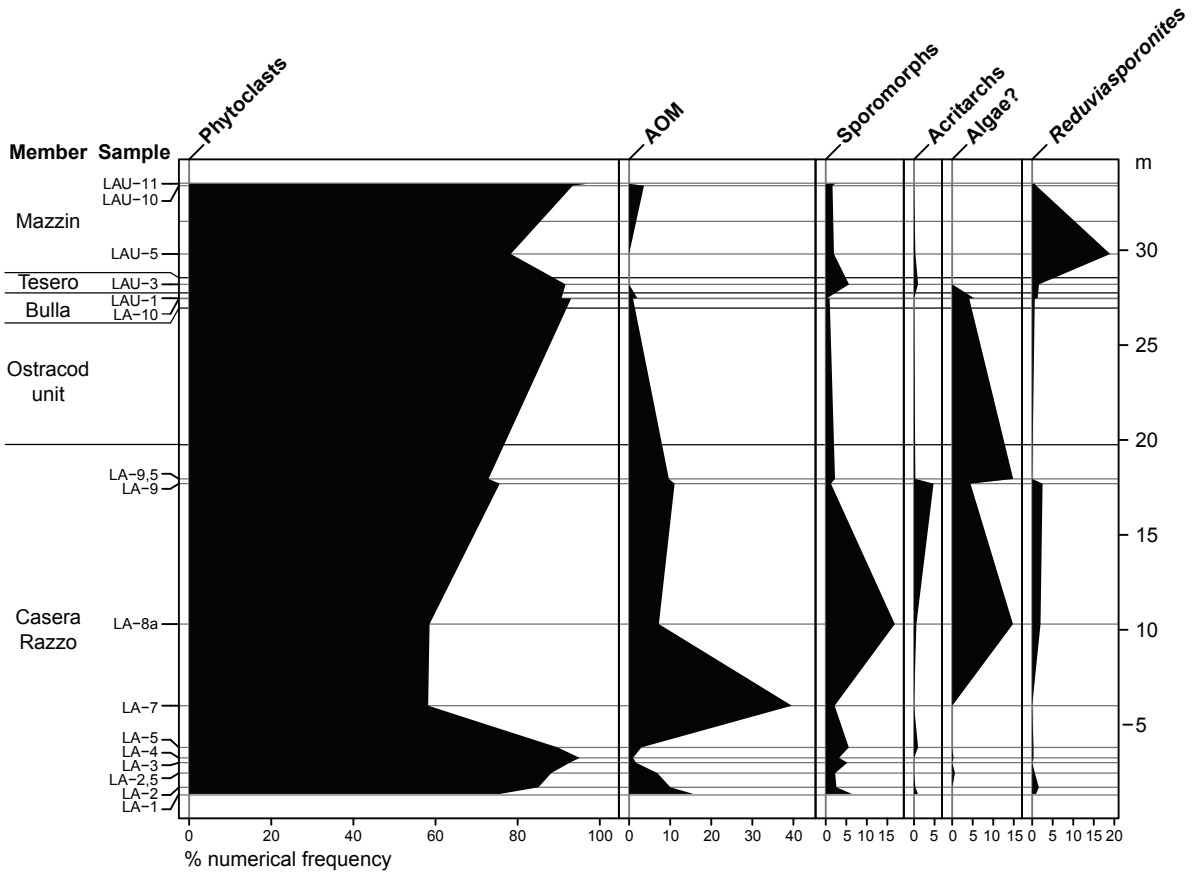

Figure 9: Palynofacies of the Laurinswand section. Plot created in R (R Core Team, 2013) using the 'analogue' package (Simpson and Oksanen, 2018).

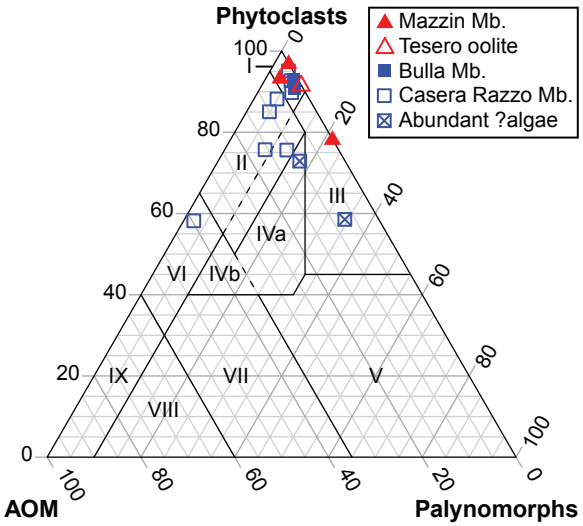

Fields:	
I	Highly proximal shelf or basin
II	Marginal dysoxic-anoxic basin
III	Heterolithic oxic shelf ('proximal shelf')
IVa	Dysoxic-suboxic shelf to basin transition
IVb	Suboxic-anoxic shelf to basin transition
V	Mud-dominated oxic shelf ('distal shelf')
VI	Proximal suboxic-anoxic shelf
VII	Distal dysoxic-anoxic 'shelf'
VIII	Distal dysoxic-oxic shelf
IX	Distal suboxic-anoxic basin

Figure 10: Ternary plot of relative abundances of phytoclasts, palynomorphs and AOM (amorphous organic matter), after Tyson (1995). Plot created in R (R Core Team, 2013) using the 'Ternary' package (Smith, 2017).

component in all samples from the Bellerophon Formation. The AOM is probably mostly derived from degraded algae and bacteria, but may also comprise strongly degraded land plant tissue. Under fluorescence, the AOM appears non-fluorescent or weakly fluorescent and often contains strongly fluorescent inclusions such as acritarchs and very small coccoid cells that most likely represent (cyano-)bacteria. Sporomorphs (in the overwhelming majority bisaccate pollen) are ubiquitous, but minor components with a relative abundance of 1–6%, except in sample 8a, where they constitute ca. 17% of the assemblage. Identifiable animal remains are extremely rare (one scolecodont – Fig. 7N – and a fragment of cuticle, presumably from a worm – Fig. 7O) and did not show up during counting. *Reduviasporonites* is present in low frequencies in all samples (<1–2.5%) with the exception of sample LAU-5 where it reaches approximately 19%. The above mentioned, unidentified putative algae are rare and not always countable (<1 %) in the lower part of the Casera Razzo Member, but occur in higher amounts (>4%) in the upper Casera Razzo and Bulla members, with peaks in abundance in samples LA-8a and LA-9,5 (both ca. 15%).

Most samples from the Werfen Formation did not deliver a sufficient amount of organic residue to allow robust quantitative palynofacies analysis or were excluded from the analysis because of heavy contamination by recent fungi. It is notable that of the four analysed samples, three (LAU-3, LAU-5, LAU-11) are completely or almost

void of AOM, with AOM also being relatively scarce in the fourth palyniferous sample (LAU-10).

A ternary AOM-phytoclast-palynomorph plot (Fig. 5; after Tyson, 1995) shows the clustering of palynofacies in fields I (indicating highly proximal shelf or basin) and II (marginal dysoxic-anoxic basin), with the exception of three samples with unusually high amounts of problematic fungal or algal palynomorphs (two from the Casera Razzo Member, one from the Mazzin Member) that are located in fields III (heterolithic, 'proximal' oxic shelf) and IVa (shelf to basin transition). This distribution is consistent with a proximal shelf setting under generally dysoxic conditions, where AOM and palynomorphs are diluted by a high input of phytoclasts. The Casera Razzo Member shows the greatest overall variation, especially in terms of AOM content relative to phytoclasts and palynomorphs. The latter can be viewed as a proxy for oxygen concentration, since AOM is more likely to be preserved under dysoxic or anoxic conditions. Samples from the Bulla, Tesero and Mazzin members all have a very low AOM content, indicating well-oxygenated waters and/or strong dilution.

4.5 Ostracods

Twelve ostracod assemblages of low to moderate species diversity have been recovered so far from the upper part of the Bellerophon Formation (Casera Razzo Member, Bulla Member) at the Laurinswand section (Fig. 5, Tab. 2). The lower Casera Razzo Member (samples LA-1, LA-3, LA-4, LA-4,5, LA-5) is mostly marked by a relatively high species diversity with taxa like *Cryptobairdia* Sohn 1960, *Bairdia* McCoy 1844, *Acratia* Delo 1930, *Hollinella* Coryell 1928, *Neoulrichia* Kozur 1981, *Parabythocythere* Kozur 1981, *Paracypris* Sars 1866 and *Paramacrocypris* Kozur 1985. Most of the assemblages here are dominated by *Sargentina postacuta* (Zalanyi 1974) (Fig. 5B), *Sulcella suprapermiana* Kozur 1985 and *Glyptopleurina pasinii* Crasquin 2008. Sample LA-2 from the lower part of the section and samples from the upper part of the Casera Razzo Member (LA-6, LA-9 and LA-9,5) show a predominace of *S. postacuta* and low diversity. The assemblage of LA-8a consists exclusively of *Cavellina bellerophonella* and *S. postacuta*. Sample LA-10, which was taken from the uppermost Bellerophon Formation (Bulla Member), is dominated by *Bairdia cheni* Crasquin 2008.

5. Discussion

5.1 Permian–Triassic boundary

In the Southern Alps, the Tesero Member is generally used as a proxy for the PTB, but the actual boundary may lie within the Tesero Member or the lower part of the Mazzin Member, which are interfingering. In the Pufels/Bulla section, the boundary was located at the base of the Mazzin Member, above the lower part of the Tesero Member (an upper part is intercalated with the Mazzin

Ostracod taxa	Samples LA-											
	1	2	2,5	3	4	4,5	5	6	8a	9	9,5	10
	Casera Razzo Mb.											Bu.
Sulcella sp.	X											
Acratia sp.1	X	X		X	X		X					
Sulcella suprapermiana Kozur 1985	X	X	X	X	X	X	X					
Paraparchitidae	X		X				X					
Paramacrocypris schallreuteri Kozur 1985	X			X	X	X	X	X				
Hollinella sp.	X			X	X	X	X				X	
Acratia spp.	X					X	X	X		X		
Cavellina bellerophonella Crasquin 2008	X	X		X				X	X	X	X	
Bairdia cheni Crasquin 2008	X			X	X	X	X					X
Glyptopleurina pasinii Crasquin 2008	X	X	X	X	X	X	X					X
Sargentina postacuta (Zalanyi 1974)	X	X	X	X	X	X	X	X	X	X	X	X
Cavellina sp. cf. *C. triassica* Crasquin 2008		X		X								
Cavellina sp.		X			X		X			X	X	X
Cavellina sp. cf. *C. alpina* Crasquin 2008				X								
Neoulrichia pulchra Kozur 1981				X	X	X	X					
Cypridoidae spp.					X							
Parabythocythere sp. 1					X							
Bairdiacypris spp.						X	X	X				
Paracypris sp.							X					
Cryptobairdia bellerophonella Mette & Roozbahani 2012								X				

Table 2: Preliminary ostracod range chart of the upper Bellerophon Formation at the Laurinswand section.

Member), by the first occurrence of *Hindeodus parvus* (Farabegoli et al., 2007). Boschetti (2010) located the PTB in the Laurinswand section approximately at the top of the section in the present study, within the Mazzin Member. This was based on $\delta^{13}C$ carbon isotope values showing a minimum at this position following a negative shift that starts in the uppermost Bellerophon Formation. Such a negative shift has been found in many PTB sections, including in the Southern Alps, and is considered to be linked to the extinction event, while the following first minimum in $\delta^{13}C$ is often used as a proxy for the PTB (Horacek et al., 2010; Korte and Kozur, 2010, and references therein; Brand et al., 2012; Kraus et al., 2013). The increased relative abundance of *Reduviasporonites* in the lower Mazzin Member at the Laurinswand section might be related to preservational bias, considering the low total amount of organic residue in the respective rock sample, but might also correspond to the "fungal spike" in the Tesero Member at its type locality, which would be consistent with the PTB being located above the Tesero Member at the Laurinswand.

5.2 Biological affinities of spores and pollen

The palynological record from the Laurinswand section allows us to reconstruct a diverse flora with all major plant groups represented. *Lundbladispora* Balme 1963 is known from Early Triassic Isoetales, e.g., *Isoetes beestoni* Retallack 1997, but the form-genus may also include microspores with a selaginelloid affinity (Balme, 1995; Retallack, 1997). Also assignable to the lycophytes are *Densosporites*, *Kraeuselisporites*, *Lycospora*, *Playfordiaspora* (Balme, 1995; Raine et al., 2011) and other cavate spores. *Converrucosisporites* Potonié et Kremp 1954 is generally attributed to the modern fern family Dicksoniaceae (Balme, 1995), of which the first appearance in the macrofossil record lies in the Triassic (Taylor et al., 2009). *Leiotriletes* Naumova ex Potoniè et Kremp 1954 has been reported from the early fern-like plant order Zygopteridales and in the fern family Botryopteriaceae (Balme, 1995), two typical Palaeozoic groups. *Deltoidospora* Danzé-Corsin et Laveine 1963, on the other hand, is widely considered an ubiquitarian fern spore (Balme, 1995). *Calamospora* is attributable to sphenophytes (Balme, 1995; Kelber and Van Konijnenburg-van Cittert, 1997).

Most bisaccate pollen types (*Falcisporites*, *Gardenasporites* Klaus 1963, *Klausipollenites*, *Lunatisporites*, *Platysaccus* Potonié et Klaus 1954, *Protohaploxypinus* Samoilovitch 1953, *Strotersporites* Wilson 1962, *Vitreisporites* Leschik 1955) can be attributed to conifers and/or pteridosperms (Townrow, 1962; Clement-Westerhof, 1974; Traverse, 1988; Balme, 1995; Looy et al., 2001). Some forms are known from *in situ* finds, which makes a more detailed botanical attribution possible. *Lueckisporites*-type pollen has been found *in situ* in the Southern Alps in *Majonica alpina* Clement-Westerhof 1987, but has been associated with other conifers as well (Clement-Westerhof 1987; Meyen, 1997). Prepollen like *Nuskoisporites* has also been found *in situ* in the Southern Alps, and can therefore be assigned to *Ortiseia* Florin 1964 (Clement-Westerhof, 1987). *Illinites* belongs to various species of voltziacean conifers (e.g., Grauvogel-Stamm, 1978). *Jugasporites* was produced in the Permian by the Ullmanniaceae (Balme, 1995), but was also found *in situ* in the Triassic male cones of *Voltzia recubariensis* (Massalongo ex De Zigno) Schenk 1868 (Brack and Kustatscher, 2013). *Paravesicaspora* Klaus 1963 and *Vittatina* belong to the seed fern order Peltaspermales (Looy and Hotton, 2014). The rare monocolpate pollen *Cycadopites* may belong to the ginkgophytes or cycadophytes (e.g., Kustatscher et al., 2010; Looy and Hotton, 2014). *Ephedripites* is morphologically similar to the pollen of extant *Ephedra* Linnaeus 1753 and therefore attributed to the Gnetales (Balme, 1995).

Thus, the flora appears to be dominated by conifer and seed fern (mostly Peltaspermales) taxa, with rare lycophytes, ferns, sphenophytes and putative ginkgophytes, cycadophytes and Gnetales. By comparing this with the stratigraphically closest macroflora from the Dolomites, the Wuchiapingian Bletterbach flora, several differences become evident. The Wuchiapingian floras of the Dolomites in general are dominated by conifers (with the exception of the Bletterbach megafossil horizon), which is in agreement with the palynological data. Ginkgophytes, a common to dominant plant group in the Bletterbach flora (particularly in the megafossil horizon; Kustatscher et al., 2017a, b), were not identified in the palynological assemblages of the Bletterbach successions, yet are probably represented in the Laurinswand palynoflora by occasional *Cycadopites*. Seed ferns, cycadophytes and horsetails are rare elements among the macroremains, whereas several of the abundant bisaccate pollen were probably produced by seed ferns. The lycophytes, represented in the palynological record by *Playfordiaspora*, *Lycospora* and other types of spores, are missing in the Lopingian macrofloras of the Dolomites (Kustatscher et al., 2017a, b). Regarding the putative Gnetales in the palynological record, the oldest confidently identified gnetalean macroremains documented so far come from the Lower Cretaceous, although putative cases have been found in the Permian and Triassic (Taylor et al., 2009).

The comparison between the Bletterbach macro- and palynoflora evidences the differences between the macro- and microfossil records and how the macrofloral record can be deficient in capturing regional floral diversity. The macrofossil record is most likely to represent plants growing in relatively close proximity to the depositional site, whereas sporomorphs are transported by wind and water from a wide range of environments, including extrabasinal habitats unsuitable for plant macrofossil preservation (Kustatscher et al., 2017a). The high diversity among the saccate pollen species and genera points to the existence of plant communities characterized by conifers and/or seed ferns still unknown from the macrofloral record. This includes *Jugasporites delasaucei*, a pollen species found *in situ* in cones of *Ullmannia frumentaria* (Schlotheim) Göppert 1850, a taxon not yet

identified in the Dolomites. On the other hand, the abundance of ginkgoalean macrofossils is in contrast with the rarity of pollen assignable to the ginkgophytes, such as *Cycadopites* (Kustatscher et al., 2017b). The sporomorph record therefore may not represent accurately the local flora, and in many cases, questions remain about the precise affinities.

5.3 Reduviasporonites *Wilson 1962*

A mass occurrence of *Reduviasporonites* (al. *Tympanicysta* Balme 1980, *Chordecystia* Foster 1979) has been observed in the Tesero Member, close to the PTB, in the Tesero section of the Southern Alps (Eshet et al., 1995; Visscher et al., 1996; Foster et al., 2002). Similar observations have been made in other parts of the world in approximately coeval strata (Eshet et al., 1995; Steiner et al., 2003; Sandler et al., 2006; Rampino and Eshet, 2018; comp. Bercovici et al., 2015; Bercovici and Vajda, 2016; Hochuli, 2016; Cui et al., 2017). This phenomenon has been called a "fungal spike" and led to theories about the role that this taxon might have played in the end-Permian mass extinction as a saprophyte or pathogen. These theories are based on the interpretation that *Reduviasporonites* represents fungi (Eshet et al., 1995; Visscher et al., 1996, 2011; Elsik, 1999), but it has also been interpreted as an alga (Afonin et al., 2001; Foster et al., 2002), and its affinity is still unresolved (Sephton et al., 2009).

In the Laurinswand section, *Reduviasporonites* is present in almost all palynological assemblages from the upper Bellerophon and lowermost Werfen formations. Sample LAU-5 contains an anomalously high amount of *Reduviasporonites* (19%; Fig. 8). This is still far less than the almost exclusive presence of this taxon in the Tesero Member at the Tesero section, but such a mass occurrence is not evident in the Tesero Member at the Laurinswand section. Since the Mazzin and Tesero members are partly coeval, it is possible that LAU-5 represents a local expression of the same "fungal spike" observed in the latter section. However, in the Laurinswand section an increase in spores precedes the so-called "fungal spike", reversed from the original model when the "fungal spike" was introduced (Eshet et al., 1995). Of course, there may well have been more than one mass occurrence of *Reduviasporonites*. The palynology of the Werfen Formation is still insufficiently studied to make this determination. In our material, the relatively high abundance of *Reduviasporonites* is also connected to a low total yield of particulate organic matter and is therefore potentially a taphonomic signal.

5.4 Palaeoenvironments

The five MF types (see 4.2) recorded in the upper Bellerophon Formation at the Laurinswand section represent an inner ramp setting with partly restricted and partly open marine conditions. The stratigraphic succession of the MF types (Fig. 2), as well as the general lithostratigraphy and lithofacies reflect three cycles of sea level change (see Neri, 2007a; Posenato, 2019); a transgressive-regressive development in the lower Casera Razzo Member (Lo4: 0–13.1 m above the base of the section), another transgressive-regressive trend in the upper Casera Razzo Member and the Ostracod unit (Lo5: 13.1–27 m), and a transgressive event in the Bulla Member (Sc1: 27–27.7 m).

The presence of MF type A at the base of the section and in the upper part of the Casera Razzo Member respectively indicates a turbulent, open-marine environment at the base of a transgressive-regressive cycle (Lo4 and Lo5, respectively). It is succeeded in both cases by MF types (B–E) indicating more restricted, lagoonal conditions during the highstand and regression phases. The highstands are marked by increased deposition of shaly/marly layers. The presence of high amounts of fine-grained siliciclastics indicates a less turbulent, protected depositional environment compared to the arenitic sand shoals of MF type A. The lower, transgressive part of Lo5 is marked by abundant algae and corresponds to the Algae assemblage of Broglio Loriga et al. (1988). The overlying Ostracod unit is considered regressive (Farabegoli et al., 2007). The start of a new transgression (Sc1) in the overlying Bulla Member is indicated by the transition from MF type D (restricted) to MF type B (transition restricted to open-marine) and by the termination of dolomitization. The base of the Bulla Member is generally marked by an unconformity/paraconformity (Farabegoli et al., 2007), which is not conspicuous at the Laurinswand section. Sequence Sc1 also encompasses the Tesero and Mazzin members, although the contact between the Bulla and Tesero members is regarded as another unconformity/paraconformity (Farabegoli et al., 2007; Neri, 2007a; Posenato, 2019).

The ostracod assemblages from the Casera Razzo Member, Ostracod unit and Bulla Member are also indicative of two transgressive-regressive developments within the upper Bellerophon Formation and a transgressive trend in the Bulla Member. The presence of normal marine ostracod taxa and relatively high species diversity in samples LA-1, LA-3, LA-4, LA-4,5 and LA-5 suggest more or less normal marine conditions in the lower Casera Razzo Member. However, several samples (LA-2, LA-6, LA-8a, LA-9 and LA-9,5) show a lower diversity and a predominance of *Sargentina postacuta* Zalanyi 1974 and (except for LA-2) *Cavellina bellerophonella* Crasquin 2008, which have been interpreted as eurytopic species with great tolerance to adverse environmental conditions such as salinity deviations or oxygen deficiency (Crasquin et al., 2008). These samples may therefore reflect unfavourable environmental conditions in terms of salinity or oxygen concentration. The assemblages of LA-6, LA-8a, LA-9 and LA-9,5 are strongly dominated by these two species or just *S. postacuta* and are therefore a strong indicator of environmental deterioration in the middle and upper part of the Casera Razzo Member. By contrast, an assemblage from the Bulla Member is dominated by *Bairdia cheni* Crasquin 2008. The Bairdioidea, which are

represented by this species, usually occur in open marine, well-oxygenated environments. Their abundant presence thus indicates normal marine conditions. Deposition in well-oxygenated waters is also indicated by palynofacies for the analysed samples from the Werfen Formation.

The palynomorph assemblages of the Bellerophon Formation indicate a diverse flora dominated by conifers and seed ferns. A change in floras is documented in the Tesero Member by the notable (but due to low yield not robustly quantifiable) increase in spores and particularly spore tetrads. This is a common feature of palynological assemblages from this time (Looy et al., 1999, 2001, 2005; Hochuli et al., 2010; Hermann et al., 2011) and has also been found before in the Dolomites at Tramin/Termeno (Looy et al., 2005). The base of the Tesero Member is generally considered to represent the main extinction event of the end-Permian mass extinction in the Dolomites, and the high amount of spore tetrads and generally higher spore/pollen ratio at this position in the stratigraphy has been linked to a disaster flora dominated by lycopsids (Looy et al., 1999). A proposed cause for the increased production of permanent tetrads (and at the same time of malformed pollen grains) is high UV-B radiation due to the extensive volcanic activity at that time (Visscher et al., 2004; Benca et al., 2018). In the case of the Laurinswand, the yield was insufficient for a meaningful analysis of the spore/pollen ratio, and the few tetrads are too poorly preserved for a more specific identification, but the observed pattern is consistent with records from other localities, even under these constraints.

6. Conclusions

The occurrence of relatively high amounts of *Reduviasporonites* in a sample from the Mazzin Member and absence of a spike in the abundance of this taxon in the Tesero Member at the Laurinswand section suggests that there may be multiple, possibly local mass occurrences in the Werfen Formation, rather than a single "fungal spike". This signal would then not be suitable as a basis for regional or interregional correlation. Another question remains about whether an actual extinction is reflected in the palynomorphs (see also Nowak et al., 2019). The palynomorph assemblages from the Werfen Formation that we studied here were quantitatively limited and consequently not fully representative, but strikingly, they contained various pollen taxa that were present in the Bellerophon Formation, beside the increase in spores, and without evidence of reworking.

The comparison of palynofloras and ostracod faunas shows that elevated amounts of possible algae or fungi in the palynofacies coincide with impoverished ostracod faunas indicating a deteriorated environment. The microfacies of adjacent limestone beds also indicates restricted conditions in these cases. The different data sources thus complement each other, and further comparative studies should provide more insights into their connections, but also their respective constraints, which are required for an informed interpretation.

Acknowledgements

This study was supported by the Euregio Science Fund (call 2014, IPN16: *The end-Permian mass extinction in the Southern and Eastern Alps: extinction rates vs taphonomic biases in different depositional environments*) of the Europaregion/Euregio Tirol-Südtirol-Trentino/Tirolo-Alto Adige-Trentino. Marco Pantaloni (Geological Survey of Italy), Paolo Ferretti and Riccardo Tomasoni (both MUSE, Trento) took part in logging the section. Parvin Mohtat-Aghai (University Innsbruck) processed the ostracod samples. Karl Krainer (University Innsbruck) photographed the thin sections. Herwig Prinoth (Museum Ladin) and Piero Gianolla (University of Ferrara) commented on the regional geology. We thank Sylvie Crasquin and an anonymous reviewer for their helpful feedback.

References

Afonin, S.A., Barinova, S.S., Krassilov, V.A., 2001. A bloom of *Tympanicysta* Balme (green algae of zygnematalean affinities) at the Permian–Triassic boundary. Geodiversitas, 23/4, 481–487.

Algeo, T.J., Chen, Z.-Q., Bottjer, D.J., 2015. Global review of the Permian–Triassic mass extinction and subsequent recovery: Part II. Earth-Science Reviews, 149, 1–4. https://doi.org/10.1016/j.earscirev.2015.09.007

Balme, B.E., 1995. Fossil in situ spores and pollen grains: an annotated catalogue. Review of Palaeobotany and Palynology, 87, 81–323. https://doi.org/10.1016/0034-6667(95)93235-X

Benca, J.P., Duijnstee, I.A.P., Looy, C.V., 2018. UV-B–induced forest sterility: Implications of ozone shield failure in Earth's largest extinction. Science Advances, 4/2, e1700618. https://doi.org/10.1126/sciadv.1700618

Benton, M.J., Newell, A.J., 2014. Impacts of global warming on Permo-Triassic terrestrial ecosystems. Gondwana Research, 25/4, 1308–1337. https://doi.org/10.1016/j.gr.2012.12.010

Benton, M.J., Twitchett, R.J., 2003. How to kill (almost) all life: the end-Permian extinction event. Trends in Ecology & Evolution, 18/7, 358–365. https://doi.org/10.1016/S0169-5347(03)00093-4

Benton, M.J., Tverdokhlebov, V.P., Surkov, M.V., 2004. Ecosystem remodelling among vertebrates at the Permian–Triassic boundary in Russia. Nature, 432, 97–100. https://doi.org/10.1038/nature02950

Bercovici, A., Cui, Y., Forel, M.-B., Yu, J., Vajda, V., 2015. Terrestrial paleoenvironment characterization across the Permian–Triassic boundary in South China. Journal of Asian Earth Sciences, 98, 225–246. https://doi.org/10.1016/j.jseaes.2014.11.016

Bercovici, A., Vajda, V., 2016. Terrestrial Permian – Triassic boundary sections in South China. Global and Planetary Change, 143, 31–33. https://doi.org/10.1016/j.gloplacha.2016.05.010

Boschetti, F., 2010. Sedimentologische und Geochemische Untersuchung der Bellerophon- und

Werfen-Formation im Raum Westliche Dolomiten. Unpublished Diploma Thesis, University of Innsbruck, Innsbruck, Austria, 78 pp.

Brack, P., Kustatscher, E., 2013. *Voltzia recubariensis* from the uppermost Angolo Limestone of the Bagolino succession (Southern Alps of Eastern Lombardy, Italy). Geo. Alp, 10, 61–70.

Brand, U., Posenato, R., Came, R., Affek, H., Angiolini, L., Azmy, K., Farabegoli, E., 2012. The end-Permian mass extinction: A rapid volcanic CO_2 and CH_4-climatic catastrophe. Chemical Geology, 322–323, 121–144. https://doi.org/10.1016/j.chemgeo.2012.06.015

Brandner, R., Horacek, M., Keim, L., Scholger, R., 2009. The Pufels/Bulla road section: Deciphering environmental changes across the Permian-Triassic boundary to the Olenekian by integrated litho-, magneto- and isotope stratigraphy. A field trip guide. Geo.Alp, 6, 116–132.

Broglio Loriga, C., Góczán, F., Haas, J., Lenner, K., Neri, C., Oravecz-Scheffer, A., Posenato, R., Szabo, I., Tóth-Makk, Á., 1990. The Lower Triassic sequences of the Dolomites (Italy) and Transdanubian mid-mountains (Hungary) and their correlation. Memorie di Scienze Geologiche, 42, 41–103.

Broglio Loriga, C., Neri, C., Pasini, M., Posenato, R., 1988. Marine fossil assemblages from Upper Permian to lowermost Triassic in the Western Dolomites (Italy). Memorie della Società Geologica Italiana, 34, 5–44.

Chen, Z.-Q., Algeo, T.J., Bottjer, D.J., 2014. Global review of the Permian–Triassic mass extinction and subsequent recovery: Part I. Earth-Science Reviews, 137, 1–5. https://doi.org/10.1016/j.earscirev.2014.05.007

Cirilli, S., Pirini Radrizzani, C., Ponton, M., Radrizzani, S., 1998. Stratigraphical and palaeoenvironmental analysis of the Permian–Triassic transition in the Badia Valley (Southern Alps, Italy). Palaeogeography, Palaeoclimatology, Palaeoecology, 138, 85–113. https://doi.org/10.1016/S0031-0182(97)00123-5

Clement-Westerhof, J.A., 1974. In situ pollen from gymnospermous cones from the Upper Permian of the Italian Alps — A preliminary account. Review of Palaeobotany and Palynology, 17, 63–73. https://doi.org/10.1016/0034-6667(74)90092-X

Clement-Westerhof, J.A., 1987. Aspects of Permian palaeobotany and palynology, VII. The Majonicaceae, a new family of Late Permian conifers. Review of Palaeobotany and Palynology, 52, 375–402. https://doi.org/10.1016/0034-6667(87)90066-2

Crasquin, S., Perri, M.C., Nicora, A., De Wever, P., 2008. Ostracods across the Permian-Triassic boundary in Western Tethys: the Bulla parastratotype (Southern Alps, Italy). Rivista Italiana di Paleontologia e Stratigrafia, 114/2, 233–262.

Cui, Y., Bercovici, A., Yu, J., Kump, L.R., Freeman, K.H., Su, S., Vajda, V., 2017. Carbon cycle perturbation expressed in terrestrial Permian–Triassic boundary sections in South China. Global and Planetary Change, 148, 272–285. https://doi.org/10.1016/j.gloplacha.2015.10.018

Elsik, W.C., 1999. *Reduviasporonites* Wilson 1962: Synonymy of the fungal organism involved in the late Permian crisis. Palynology, 23/1, 37–41. https://doi.org/10.1080/01916122.1999.9989519

Erwin, D.H., 1994. The Permo-Triassic extinction. Nature, 367, 231–236. https://doi.org/10.1038/367231a0

Eshet, Y., Rampino, M.R., Visscher, H., 1995. Fungal event and palynological record of ecological crisis and recovery across the Permian-Triassic boundary. Geology, 23/11, 967–970.

Farabegoli, E., Perri, M.C., Posenato, R., 2007. Environmental and biotic changes across the Permian–Triassic boundary in western Tethys: The Bulla parastratotype, Italy. Global and Planetary Change, 55, 109–135. https://doi.org/10.1016/j.gloplacha.2006.06.009

Flügel, E., 2004. Microfacies of carbonate rocks: analysis, interpretation and application. Springer Verlag, Berlin, Heidelberg, 984 pp.

Foster, W.J., Danise, S., Price, G.D., Twitchett, R.J., 2017. Subsequent biotic crises delayed marine recovery following the late Permian mass extinction event in northern Italy. PLOS ONE, 12/3, e0172321. https://doi.org/10.1371/journal.pone.0172321

Foster, C.B., Stephenson, M.H., Marshall, C., Logan, G.A., Greenwood, P.F., 2002. A revision of *Reduviasporonites* Wilson 1962: Description, illustration, comparison and biological affinities. Palynology, 26/1, 35–58. https://doi.org/10.2113/0260035

Grauvogel-Stamm, L., 1978. La Flore du Grès à Voltzia (Buntsandstein supérieur) des Vosges du Nord (France): Morphologie, Anatomie, Interprétations Phylogénique et Paléogéographique. Sciences Géologiques, Mémoire 50, Institut de Géologie, Strasbourg, France, 225 pp.

Grenfell, H.R., 1995. Probable fossil zygnemataceae algal spore genera. Review of Palaeobotany and Palynology, 84, 201–220. https://doi.org/10.1016/0034-6667(94)00134-6

Groves, J.R., Rettori, R., Payne, J.L., Boyce, M.D., Altiner, D., 2007. End-Permian mass extinction of lagenide foraminifers in the Southern Alps (northern Italy). Journal of Palaeontology, 81/3, 415–434. https://doi.org/10.1666/05123.1

Hermann, E., Hochuli, P.A., Bucher, H., Brühwiler, T., Hautmann, M., Ware, D., Roohi, G., 2011. Terrestrial ecosystems on North Gondwana following the end-Permian mass extinction. Gondwana Research, 20, 630–637. https://doi.org/10.1016/j.gr.2011.01.008

Hochuli, P.A., 2016. Interpretation of "fungal spikes" in Permian-Triassic boundary sections. Global and Planetary Change, 144, 48–50. https://doi.org/10.1016/j.gloplacha.2016.05.002

Hochuli, P.A., Hermann, E., Vigran, J.O., Bucher, H., Weissert, H., 2010. Rapid demise and recovery of plant ecosystems across the end-Permian extinction event. Global and Planetary Change, 74, 144–155. https://doi.org/10.1016/j.gloplacha.2010.10.004

Hofmann, R., Goudemand, N., Wasmer, M., Bucher, H., Hautmann, M., 2011. New trace fossil evidence

for an early recovery signal in the aftermath of the end-Permian mass extinction. Palaeogeography, Palaeoclimatology, Palaeoecology, 310, 216–226. https://doi.org/10.1016/j.palaeo.2011.07.014

Hofmann, R., Hautmann, M., Brayard, A., Nützel, A., Bylund, K.G., Jenks, J.F., Vennin, E., Olivier, N., Bucher, H., 2014. Recovery of benthic marine communities from the end-Permian mass extinction at the low latitudes of eastern Panthalassa. Palaeontology, 57/3, 547–589. https://doi.org/10.1111/pala.12076

Hofmann, R., Hautmann, M., Bucher, H., 2015. Recovery dynamics of benthic marine communities from the Lower Triassic Werfen Formation, northern Italy. Lethaia, 48/4, 474–496. https://doi.org/10.1111/let.12121

Horacek, M., Povoden, E., Richoz, S., Brandner, R., 2010. High-resolution carbon isotope changes, litho- and magnetostratigraphy across Permian-Triassic Boundary sections in the Dolomites, N-Italy. New constraints for global correlation. Palaeogeography, Palaeoclimatology, Palaeoecology, 290, 58–64. https://doi.org/10.1016/j.palaeo.2010.01.007

Jansonius, J., 1962. Palynology of Permian andTriassic sediments, Peace River area, western Canada. Palaeontographica Abteilung B, 110, 35–98.

Kearsey, T., Twitchett, R.J., Price, G.D., Grimes, S.T., 2009. Isotope excursions and palaeotemperature estimates from the Permian/Triassic boundary in the Southern Alps (Italy). Palaeogeography, Palaeoclimatology, Palaeoecology, 279, 29–40. https://doi.org/10.1016/j.palaeo.2009.04.015

Kelber, K.-P., Van Konijnenburg-van Cittert, J.H.A., 1998. *Equisetites arenaceus* from the Upper Triassic of Germany with evidence for reproductive strategies. Review of Palaeobotany and Palynology, 100/1, 1–26. https://doi.org/10.1016/S0034-6667(97)00061-4

Klaus, W., 1963. Sporen aus dem südalpinen Perm (Vergleichsstudie für die Gliederung nordalpiner Salzserien). Jahrbuch der Geologischen Bundesanstalt, 106, 229–361.

Knoll, A.H., Bambach, R.K., Payne, J.L., Pruss, S., Fischer, W.W., 2007. Paleophysiology and end-Permian mass extinction. Earth and Planetary Science Letters, 256/3, 295–313. https://doi.org/10.1016/j.epsl.2007.02.018

Koeberl, C., Farley, K.A., Peucker-Ehrenbrink, B., Sephton, M.A., 2004. Geochemistry of the end-Permian extinction event in Austria and Italy: No evidence for an extraterrestrial component. Geology, 32, 1053–1056. https://doi.org/10.1130/G20907.1

Korte, C., Kozur, H.W., 2010. Carbon-isotope stratigraphy across the Permian–Triassic boundary: A review. Journal of Asian Earth Sciences, 39, 215–235. https://doi.org/10.1016/j.jseaes.2010.01.005

Kraus, S.H., Brandner, R., Heubeck, C., Kozur, H.W., Struck, U., Korte, C., 2013. Carbon isotope signatures of latest Permian marine successions of the Southern Alps suggest a continental runoff pulse enriched in land plant material. Fossil Record, 16/1, 97–109. https://doi.org/10.1002/mmng.201300004

Kustatscher, E., Bernardi, M., Petti, F.M., Franz, M., Van Konijnenburg-van Cittert, J.H.A., Kerp, H., 2017a. Sea-level changes in the Lopingian (late Permian) of the northwestern Tethys and their effects on the terrestrial palaeoenvironments, biota and fossil preservation. Global and Planetary Change, 148, 166–180. https://doi.org/10.1016/j.gloplacha.2016.12.006

Kustatscher, E., Van Konijnenburg-van Cittert, J.H.A., Looy, C.V., Labandeira, C.C., Wappler, T., Butzmann, R., Fischer, T.C., Krings, M., Kerp, H., Visscher, H., 2017b. The Lopingian (late Permian) flora from the Bletterbach Gorge in the Dolomites, Northern Italy: a review. Geo.Alp, 14, 39–61.

Kustatscher, E., Van Konijnenburg-van Cittert, J.H.A., Roghi, G., 2010. Macrofloras and palynomorphs as possible proxies for palaeoclimatic and palaeoecological studies: A case study from the Pelsonian (Middle Triassic) of Kühwiesenkopf/Monte Prà della Vacca (Olang Dolomites, N-Italy). Palaeogeography, Palaeoclimatology, Palaeoecology, 290, 71–80. https://doi.org/10.1016/j.palaeo.2009.07.001

Looy, C.V., Hotton, C.L., 2014. Spatiotemporal relationships among Late Pennsylvanian plant assemblages: Palynological evidence from the Markley Formation, West Texas, U.S.A. Review of Palaeobotany and Palynology, 211, 10–27. https://doi.org/10.1016/j.revpalbo.2014.09.007

Looy, C.V., Brugman, W.A., Dilcher, D.L., Visscher, H., 1999. The delayed resurgence of equatorial forests after the Permian–Triassic ecologic crisis. Proceedings of the National Academy of Sciences, 96/24, 13857–13862. https://doi.org/10.1073/pnas.96.24.13857

Looy, C.V., Collinson, M.E., Van Konijnenburg-van Cittert, J.H.A., Visscher, H., Brain, A.P.R., 2005. The ultrastructure and botanical affinity of end-Permian spore tetrads. International Journal of Plant Sciences, 166/5, 875–887. https://doi.org/10.1086/431802

Looy, C.V., Twitchett, R.J., Dilcher, D.L., Van Konijnenburg-van Cittert, J.H.A., Visscher, H., 2001. Life in the end-Permian dead zone. Proceedings of the National Academy of Sciences, 98/14, 7879–7883. https://doi.org/10.1073/pnas.131218098

Massari, F., Conti, M.A., Fontana, D., Helmold, K., Mariotti, N., Neri, C., Nicosia, U., Ori, G.G., Pasini, M., Pittau, P., 1988. The Val Gardena sandstone and Bellerophon Formation in the Bletterbach gorge (Alto Adige, Italy): biostratigraphy and sedimentology. Memorie di Scienze Geologiche, 40, 229–273.

Massari, F., Neri, C., Pittau, P., Fontana, D., Stefani, C., 1994. Sedimentology, palynostratigraphy and sequence stratigraphy of a continental to shallow-marine rift-related succession: Upper Permian of the eastern Southern Alps (Italy). Memorie di Scienze Geologiche, 46, 119–243.

Matthews, K.J., Maloney, K.T., Zahirovic, S., Williams, S.E., Seton, M., Müller, R.D., 2016. Global plate boundary evolution and kinematics since the late Paleozoic. Global and Planetary Change, 146, 226–250. https://doi.org/10.1016/j.gloplacha.2016.10.002

Mette, W., Roozbahani, P., 2012. Late Permian (Changsingian [sic]) ostracods of the Bellerophon Formation at Seis (Siusi) (Dolomites, Italy). Journal of Micropalaeontology, 31/1, 73–87. https://doi.org/10.1144/0262-821X11-010

Meyen, S.V., 1997. Permian conifers of Western Angaraland. Review of Palaeobotany and Palynology, 96/3, 351–447. https://doi.org/10.1016/S0034-6667(96)00046-2

Neri, C., 2007a. Formazione a Bellerophon. In Cita, M.B., Abbate, E., Conti, M.A., Falorni, P., Germani, D., Groppelli, G., Manetti, P., Petti, F.M. – Carta Geologica d'Italia – 1:50.000, Catalogo delle formazioni – Unità tradizionali. Quaderni del Servizio Geologico d'Italia, Series 3, 7/7, 64-73.

Neri, C., 2007b. Formazione di Werfen. In Cita, M.B., Abbate, E., Conti, M.A., Falorni, P., Germani, D., Groppelli, G., Manetti, P., Petti, F.M. – Carta Geologica d'Italia – 1:50.000, Catalogo delle formazioni – Unità tradizionali. Quaderni del Servizio Geologico d'Italia, Series 3, 7/7, 83-96.

Noé, S.U., 1987. Facies and paleogeography of the marine Upper Permian and of the Permian-Triassic boundary in the Southern Alps (Bellerophon Formation, Tesero Horizon). Facies, 16, 89–141. https://doi.org/10.1007/BF02536749

Onorevoli, G., Farabegoli, E., 2014. Modeling the paleogeography of north-western Palaeotethys across the Permian-Triassic boundary: constraints and possible solutions. GSTF International Journal of Geological Sciences (JGS), 1/2, 39–46. https://doi.org/10.5176/2335-6774_1.2.17

Pasini, M., 1981. Nota preliminare su una fauna ad ostracodi dei livelli superiori della Formazione a Bellerophon delle Dolomiti. Rivista Italiana di Paleontologia e Stratigrafia, 87/1, 1–22.

Pittau, P., 2001. Correlation of the upper Permian sporomorph complexes of the Southern Italian Alps with the Tatarian complexes of the stratotype region. Natura Bresciana, Annuario del Museo Civico di Scienze Naturale, Brescia, Monografia, 25, 109–116.

Posenato, R., 2009. Survival patterns of macrobenthic marine assemblages during the end-Permian mass extinction in the western Tethys (Dolomites, Italy). Palaeogeography, Palaeoclimatology, Palaeoecology, 280, 150–167. https://doi.org/10.1016/j.palaeo.2009.06.009

Posenato, R., 2010. Marine biotic events in the Lopingian succession and latest Permian extinction in the Southern Alps (Italy). Geological Journal, 45, 195–215. https://doi.org/10.1002/gj.1212

Posenato, R., 2019. The end-Permian mass extinction (EPME) and the Early Triassic biotic recovery in the western Dolomites (Italy): state of the art. Bollettino della Società Paleontologica Italiana, 58, 11–34. https://doi.org/10.4435/BSPI.2019.05

R Core Team, 2013. R: A Language and Environment for Statistical Computing. R Foundation for Statistical Computing, Vienna, Austria. http://www.r-project.org/ (accessed on 22 October 2018).

Raine, J.I., Mildenhall, D.C., Kennedy, E.M., 2011. New Zealand fossil spores and pollen: an illustrated catalogue, 4th ed, GNS Science miscellaneous series, 4. http://data.gns.cri.nz/sporepollen/index.htm (accessed on 22 October 2018).

Rampino, M.R., Eshet, Y., 2018. The fungal and acritarch events as time markers for the latest Permian mass extinction: An update. Geoscience Frontiers, 9/1, 147–154. https://doi.org/10.1016/j.gsf.2017.06.005

Rampino, M.R., Prokoph, A., Adler, A.C., Schwindt, D.M., 2002. Abruptness of the end-Permian mass extinction as determined from biostratigraphic and cyclostratigraphic analyses of. In: Koeberl, C. and MacLeod, K.G. (eds.), Catastrophic Events and Mass Extinctions: Impacts and Beyond. Geological Society of America Special Papers. Geological Society of America, Boulder, Colorado, 356, pp. 415–427.

Raup, D.M., 1979. Size of the Permo-Triassic bottleneck and its evolutionary implications. Science, 206/4415, 217–218. https://doi.org/10.1126/science.206.4415.217

Retallack, G.J., 1997. Earliest Triassic origin of *Isoetes* and quillwort evolutionary radiation. Journal of Palaeontology, 71/3, 500–521. https://doi.org/10.1017/S0022336000039524

Sandler, A., Eshet, Y., Schilman, B., 2006. Evidence for a fungal event, methane-hydrate release and soil erosion at the Permian–Triassic boundary in southern Israel. Palaeogeography, Palaeoclimatology, Palaeoecology, 242, 68–89. https://doi.org/10.1016/j.palaeo.2006.05.009

Sephton, M.A., Visscher, H., Looy, C.V., Verchovsky, A.B., Watson, J.S., 2009. Chemical constitution of a Permian-Triassic disaster species. Geology, 37/10, 875–878. https://doi.org/10.1130/G30096A.1

Servais, T., Vecoli, M., Li, J., Molyneux, S.G., Raevskaya, E.G., Rubinstein, C.V., 2007. The acritarch genus *Veryhachium* Deunff 1954: Taxonomic evaluation and first appearance. Palynology, 31/1, 191–203. https://doi.org/10.1080/01916122.2007.9989642

Simpson, G.L., Oksanen, J., 2018. analogue: Analogue and Weighted Averaging Methods for Palaeoecology. https://CRAN.R-project.org/package=analogue. (accessed on 16 November 2018).

Smith, M.R., 2017. Ternary: An R package for creating ternary plots. Zenodo. https://CRAN.R-project.org/package=Ternary. (accessed on 22 October 2018). https://doi.org/10.5281/zenodo.1068996

Spina, A., Cirilli, S., Utting, J., Jansonius, J., 2015. Palynology of the Permian and Triassic of the Tesero and Bulla sections (Western Dolomites, Italy) and consideration about the enigmatic species *Reduviasporonites chalastus*. Review of Palaeobotany and Palynology, 218, 3–14. https://doi.org/10.1016/j.revpalbo.2014.10.003

Steiner, M.B., Eshet, Y., Rampino, M.R., Schwindt, D.M., 2003. Fungal abundance spike and the Permian–Triassic boundary in the Karoo Supergroup (South Africa). Palaeogeography, Palaeoclimatology, Palaeoecology, 194, 405–414. https://doi.org/10.1016/S0031-0182(03)00230-X

Taylor, E.L., Taylor, T.N., Krings, M., 2009. Paleobotany: The Biology and Evolution of Fossil Plants, 2nd Ed. Academic Press, Burlington, 1230 pp.

Torsvik, T.H., Cocks, L.R.M., 2017. Earth History and Palaeogeography. Cambridge University Press, Cambridge, UK, 317 pp.

Townrow, J.A., 1962. On some disaccate pollen grains of Permian to Middle Jurassic age. Grana Palynologica, 3/2, 13–44.

Traverse, A., 1988. Paleopalynology. Unwin Hyman Ltd., Boston, MA, USA, 600 pp.

Twitchett, R.J., 1999. Palaeoenvironments and faunal recovery after the end-Permian mass extinction. Palaeogeography, Palaeoclimatology, Palaeoecology, 154, 27–37. https://doi.org/10.1016/S0031-0182(99)00085-1

Twitchett, R.J., Wignall, P.B., 1996. Trace fossils and the aftermath of the Permo-Triassic mass extinction: evidence from northern Italy. Palaeogeography, Palaeoclimatology, Palaeoecology, 124, 137–151. https://doi.org/10.1016/0031-0182(96)00008-9

Tyson, R.V., 1995. Sedimentary Organic Matter: Organic Facies and Palynofacies. Chapman & Hall, London, UK, 615 pp.

Visscher, H., Brugman, W.A., 1986. The Permian–Triassic boundary in the Southern Alps: a palynological approach. Memorie della Società Geologica Italiana, 34, 121–128.

Visscher, H., Brinkhuis, H., Dilcher, D.L., Elsik, W.C., Eshet, Y., Looy, C.V., Rampino, M.R., Traverse, A., 1996. The terminal Paleozoic fungal event: evidence of terrestrial ecosystem destabilization and collapse. Proceedings of the National Academy of Sciences, 93/5, 2155–2158. https://doi.org/10.1073/pnas.93.5.2155

Visscher, H., Looy, C.V., Collinson, M.E., Brinkhuis, H., van Konijnenburg-van Cittert, J.H.A., Kürschner, W.M., Sephton, M.A., 2004. Environmental mutagenesis during the end-Permian ecological crisis. Proceedings of the National Academy of Sciences, 101/35, 12952–12956. https://doi.org/10.1073/pnas.0404472101

Visscher, H., Sephton, M.A., Looy, C.V., 2011. Fungal virulence at the time of the end-Permian biosphere crisis? Geology, 39/9, 883–886. https://doi.org/10.1130/G32178.1

Wignall, P.B., Twitchett, R.J., 2002. Extent, duration, and nature of the Permian-Triassic superanoxic event. In: Koeberl, C. and MacLeod, K.G. (eds.), Catastrophic Events and Mass Extinctions: Impacts and Beyond. Geological Society of America Special Papers, Geological Society of America, Boulder, Colorado, 356, pp. 395–414.

Received: 19 11 2018
Accepted: 06 08 2019

Hendrik NOWAK[1)]*, Wolfgang METTE[2)], Fabio M. PETTI[3)], Guido ROGHI[4)], Evelyn KUSTATSCHER[1),5),6)]

[1)] Museum of Nature South Tyrol, Bindergasse/Via Bottai 1, 39100 Bozen/Bolzano, Italy; e-mail: hendrik.nowak@naturmuseum.it; evelyn.kustatscher@naturmuseum.it

[2)] Department of Geology, Universität Innsbruck, Innrain 52f, 6020 Innsbruck, Austria; e-mail: wolfgang.mette@uibk.ac.at

[3)] MUSE – Museo delle Scienze di Trento, Corso del Lavoro e della Scienza 3, Trento 38122, Italy; e-mail: fabio.petti@muse.it

[4)] Istituto di Geoscienze e Georisorse - CNR, Via Gradenigo 6, Padova 35131, Italy; e-mail: guido.roghi@igg.cnr.it

[5)] Department of Earth and Environmental Sciences, Paleontology & Geobiology, Ludwig-Maximilians-Universität München, Richard-Wagner-Straße 10, 80333 München, Germany

[6)] SNSB-Bayerische Staatssammlung für Paläontologie und Geologie, Richard-Wagner-Straße 10, 80333 München, Germany

*) Corresponding author: Hendrik NOWAK